AD-A133 392 WAVE DATA ACQUISITION AND HINDCAST FOR SAGINAW BAY MICHIGAN(U) ARMY ENGINEER WATERWAYS EXPERIMENT STATION VICKSBURG MS HYDRAULICS LAB A W GARCIA ET AL. JUN 83 1/1

UNCLASSIFIED WES/TR/HL-83-14 F/G 8/8 NL

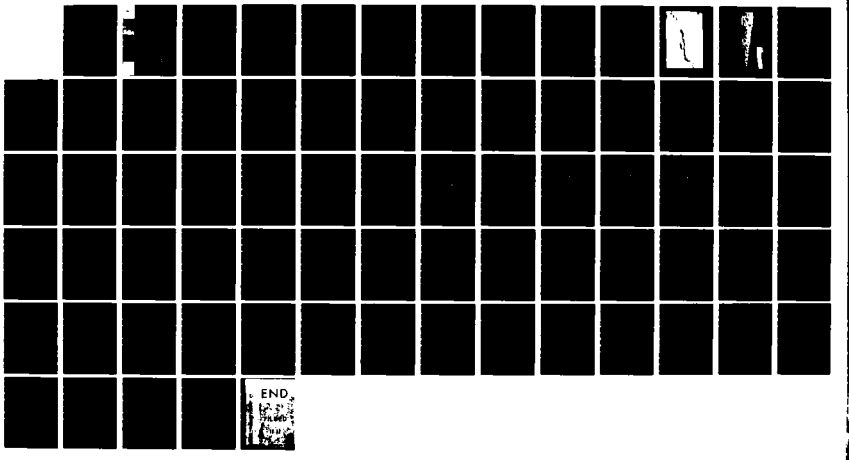

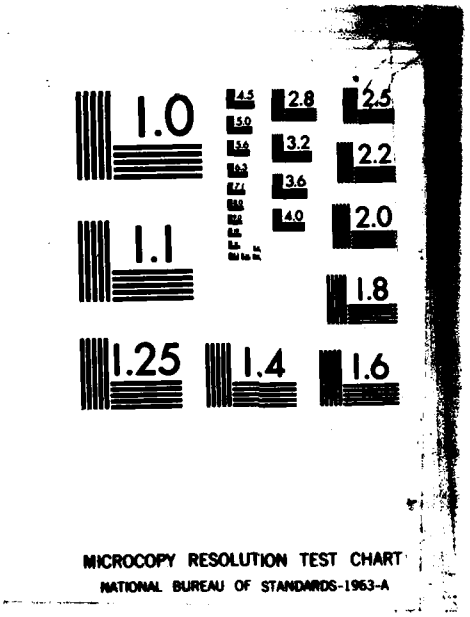
1.0
1.1
1.25
1.4
1.6
1.8
2.0
2.2
2.5
2.8
3.2
3.6
4.0
4.5
5.0
5.6
6.3
MICROCOPY RESOLUTION TEST CHART
NATIONAL BUREAU OF STANDARDS-1963-A

US Army Corps of Engineers



TECHNICAL REPORT HL-83-14

# WAVE DATA ACQUISITION AND HINDCAST FOR SAGINAW BAY, MICHIGAN

by

Andrew W. Garcia, Robert E. Jensen
Hydraulics Laboratory
U. S. Army Engineer Waterways Experiment Station
P. O. Box 631, Vicksburg, Miss. 39180

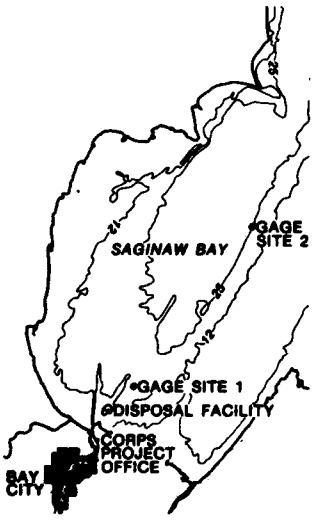


HYDRAULICS LABORATORY

June 1983
Final Report

Approved For Public Release; Distribution Unlimited



Prepared for U. S. Army Engineer District, Detroit
Detroit, Mich. 48231

Destroy this report when no longer needed. Do not return it to the originator.

The findings in this report are not to be construed as an official Department of the Army position unless so designated by other authorized documents.

The contents of this report are not to be used for advertising, publication, or promotional purposes. Citation of trade names does not constitute an official endorsement or approval of the use of such commercial products.

Unclassified

SECURITY CLASSIFICATION OF THIS PAGE (When Data Entered)

| REPORT DOCUMENTATION PAGE | READ INSTRUCTIONS BEFORE COMPLETING FORM |
|---|---|
| 1. REPORT NUMBER: Technical Report HL-83-14 | 2. GOVT ACCESSION NO.: AD-A133392 |
| | 3. RECIPIENT'S CATALOG NUMBER |
| 4. TITLE (and Subtitle): WAVE DATA ACQUISITION AND HINDCAST FOR SAGINAW BAY, MICHIGAN | 5. TYPE OF REPORT & PERIOD COVERED: Final report |
| | 6. PERFORMING ORG. REPORT NUMBER |
| 7. AUTHOR(s): Andrew W. Garcia<br>Robert E. Jensen | 8. CONTRACT OR GRANT NUMBER(s) |
| 9. PERFORMING ORGANIZATION NAME AND ADDRESS: U. S. Army Engineer Waterways Experiment Station<br>Hydraulics Laboratory<br>P. O. Box 631, Vicksburg, Miss. 39180 | 10. PROGRAM ELEMENT, PROJECT, TASK AREA & WORK UNIT NUMBERS |
| 11. CONTROLLING OFFICE NAME AND ADDRESS: U. S. Army Engineer District, Detroit<br>P. O. Box 1027<br>Detroit, Mich. 48231 | 12. REPORT DATE: June 1983<br>13. NUMBER OF PAGES: 69 |
| 14. MONITORING AGENCY NAME & ADDRESS(if different from Controlling Office) | 15. SECURITY CLASS. (of this report): Unclassified<br>15a. DECLASSIFICATION/DOWNGRADING SCHEDULE |

16. DISTRIBUTION STATEMENT (of this Report)

Approved for public release; distribution unlimited.

17. DISTRIBUTION STATEMENT (of the abstract entered in Block 20, if different from Report)

18. SUPPLEMENTARY NOTES

Available from National Technical Information Service, 5285 Port Royal Road, Springfield, Va. 22161

19. KEY WORDS (Continue on reverse side if necessary and identify by block number)

Saginaw Bay, Michigan
Water wave action
Wave data
Wave hindcast models

20. ABSTRACT (Continue on reverse side if necessary and identify by block number)

A wave-measurement system was deployed in Saginaw Bay, Michigan, for the purpose of determining the wave growth within the bay as functions of fetch and time. The wave data acquired provide the basis for development and verification of a shallow-water wave hindcast model. The hindcast model, along with 20 years of wind data, is used to perform an extremal analysis of wave conditions within Saginaw Bay. Results of the analysis show that a maximum significant wave height of about 8 ft is expected at the head of the bay.

DD FORM 1 JAN 73 1473 EDITION OF 1 NOV 65 IS OBSOLETE

Unclassified

SECURITY CLASSIFICATION OF THIS PAGE (When Data Entered)

# PREFACE

In May 1979, storm-generated waves caused significant damage to a newly completed diked dredged material disposal facility located in Saginaw Bay, Michigan. As a consequence, the U. S. Army Engineer Waterways Experiment Station (WES) was requested by the U. S. Army Engineer District, Detroit (NCE), to develop a wave-measurement system and, concurrently, a wave hindcast model in order to determine the frequency of occurrence of severe wave conditions in Saginaw Bay. Funds were authorized by NCE on 2 July 1979. The study was conducted during the period from July 1979 to February 1983 in the Wave Processes Branch, Wave Dynamics Division, Hydraulics Laboratory, WES, under the direction of Mr. H. B. Simmons, Chief of the Hydraulics Laboratory, Dr. R. W. Whalin, former Chief of the Wave Dynamics Division, and Mr. C. E. Chatham, Acting Chief of the Wave Dynamics Division.

The study was conducted under the direction of Mr. A. W. Garcia, who prepared the wave gaging portion of the report. Dr. R. E. Jensen developed the shallow-water wave hindcast model and prepared the theoretical, comparison, and design wave condition sections of the report. Also, M. B. Habeeb and B. F. Vavra coordinated all activities associated with the final publication of this report.

A special acknowledgment is due Messrs. Ernest Liebetreau and Richard Baker of the Saginaw Projects Office, CE, for their outstanding cooperation and assistance in the deployment and servicing of the wave-measurement system.

Commanders and Directors of WES during the conduct of the study and the preparation and publication of this report were COL John L. Cannon, CE, COL Nelson P. Conover, CE, and COL Tilford C. Creel, CE. Technical Director was Mr. F. R. Brown.

CONTENTS

## CONVERSION FACTORS, U. S. CUSTOMARY TO METRIC (SI) UNITS OF MEASUREMENT

U. S. customary units of measurement can be converted to metric (SI) units as follows:

| Multiply | By | To Obtain |
|---|---|---|
| acres | 4046.856 | square metres |
| cubic yards | 0.7645549 | cubic metres |
| feet | 0.3048 | metres |
| feet per second per second | 0.3048 | metres per second per second |
| knots (international) | 0.514444 | metres per second |
| miles per hour (U. S. statute) | 1.609344 | kilometres per hour |
| miles (U. S. nautical) | 1.852 | kilometres |
| miles (U. S. statute) | 1.609344 | kilometres |

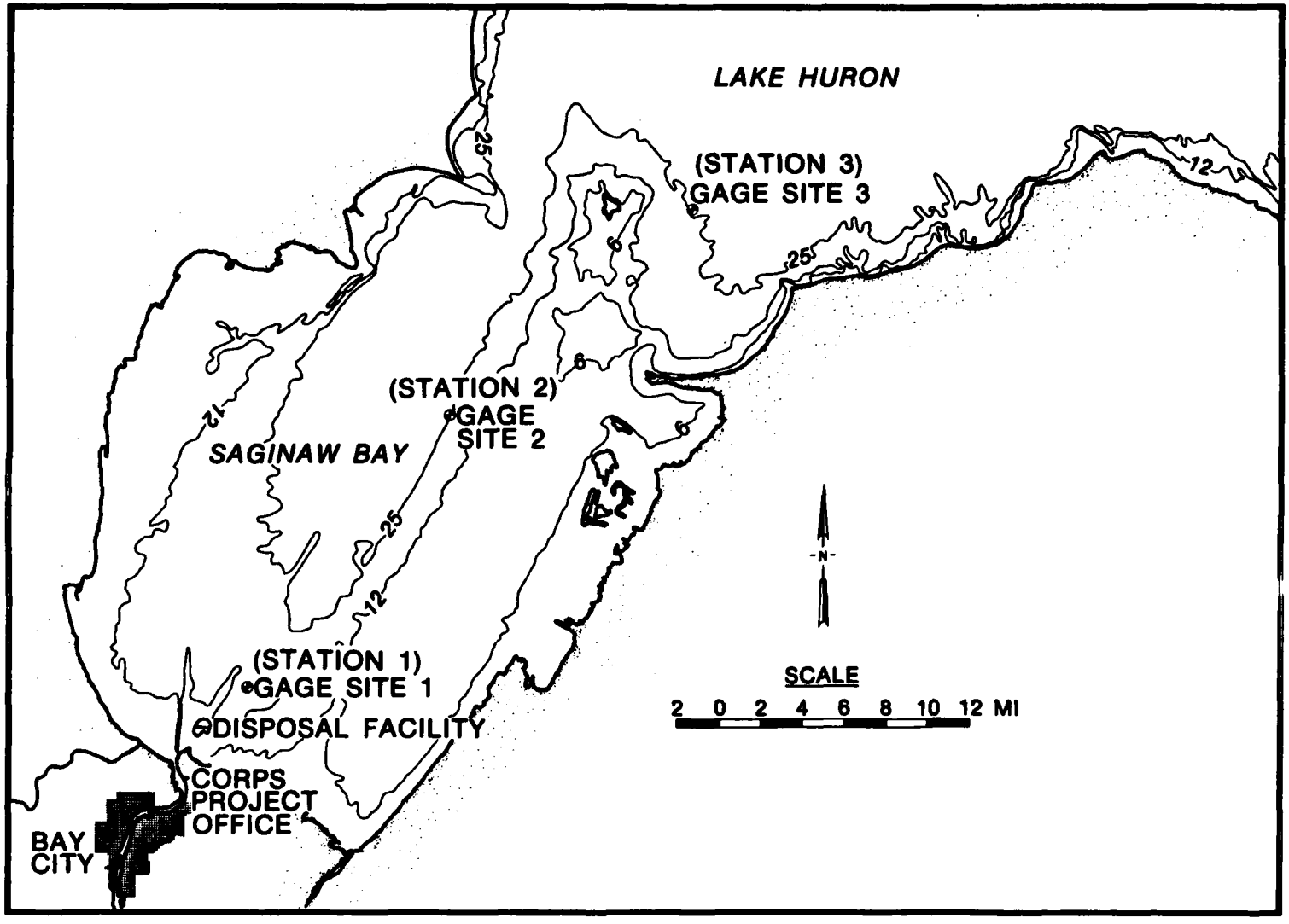


Figure 1. Saginaw Bay wave gage sites and disposal facility location

# WAVE DATA ACQUISITION AND HINDCAST FOR SAGINAW BAY, MICHIGAN

## PART I: INTRODUCTION

1. The Saginaw River is a navigable waterway that flows northward into the head of Saginaw Bay, Michigan. The areas along the river and its tributaries, the Flint, Cass, Tittabawassee, and Shiawassee Rivers, are heavily industrialized; and for years, industrial and sewage treatment wastes have been discharged into these rivers resulting in contamination of the bottom sediments. At the request of the Governor of Michigan, maintenance dredging of the lower river and Saginaw Bay navigation channel was discontinued in 1970. Dredging was suspended pending the selection of a site or construction of a containment facility suitable for disposal of the contaminated dredged material. In conjunction with the Bay County Michigan Board of Commissioners, the U. S. Army Engineer District, Detroit (NCE), selected a site to the east of the mouth of the Saginaw River as the location for construction of a diked dredged material disposal facility. Construction was begun in 1977 and completed in the fall of 1978 at a cost of about 14 million dollars. The facility covers an area of about 285 acres* in water depths of 10 to 14 ft and is protected by a rubble-mound breakwater. The design capacity is approximately 10 million cubic yards with an initial fill of 4 million cubic yards and 600,000 cubic yards yearly for 10 years, the anticipated active life of the structure. Upon filling of the facility, the resulting island will revert to Bay County Authorities, probably for recreational use. Figure 1 shows the location and scale of the structure. The cross dike was necessary for two reasons. First, construction of the structure required two building seasons. A partially completed structure would have been vulnerable to wave and ice damage during the fall and winter months. The cross dike served to close the partially completed structure while construction was suspended during the winter. Second, the dike served to support the dredge discharge pipe in order to assure uniform filling of the facility.

---

* A table of factors for converting U. S. customary units of measurements to metric (SI) units is presented on page 3.

## PART II: STORM OF MAY 1979

2. During the period 23 to 25 May 1979, a storm accompanied by sustained north to northeast winds of 30 to 35 mph produced waves that caused significant damage to the facility. The damage was confined to the northeast sector of the structure but the cost of repair and rehabilitation was in excess of one million dollars. The damage was primarily caused by waves overtopping the structure. Figure 2 is an aerial photograph taken on 25 May 1979 showing the structure being overtopped during the storm. Note the breach in the crown of the structure that had occurred prior to the photograph being taken. Figure 3 is a photograph taken on 29 May 1979, 4 days after the storm. Roughly, the same section of the structure is shown; note the damage to the crown of the structure.

3. There was conjecture following damage to the structure that although designed in accordance with guidelines of the Shore Protection Manual (U. S. Army CERC 1977) for the known weather patterns of the area, the wave climate in Saginaw Bay may have been more severe than anticipated.

4. As a consequence of damage to the structure, the NCE requested the U. S. Army Engineer Waterways Experiment Station (WES) to design and deploy a wave-measurement system in Saginaw Bay and concurrently to develop the capability of hindcasting the wave climate within the bay. The wave-measurement system was initially deployed in the fall of 1979. It was configured to provide data at two locations within the bay and one location in Lake Huron just outside the bay entrance (Figure 1). The locations referenced to Figure 1 were chosen to provide data as follows:

a. Gage Site 1. The wave climate in the vicinity of the disposal facility primarily during north and northeast winds.

b. Gage Site 2. The wave climate bayward of the shoal near the entrance to the bay during north and northeast winds. Also, by comparing the wave data at location 2 with data acquired at location 1, the wave generation (growth versus fetch and time) within the bay could be determined.

c. Gage Site 3. The wave climate just to the outside of the shoal near the entrance to the bay during north and northeast winds. By comparing the wave data at location 3 with data acquired at location 2, the amount of wave energy being transmitted across the shoal from Lake Huron to Saginaw Bay can be determined.

5. During the fall 1979, spring 1980, and fall 1981 deployments, the wave gages were set to acquire 17 min of wave data every 3 hr at a sampling

Figure 2. Disposal facility being overtopped by waves during May 1979 storm

Figure 3. Damage to disposal facility caused by May 1979 storm

rate of 2 Hz. Examination of data obtained during minor storms occurring in these deployment periods revealed there could be substantial changes in the wave climate between 3-hr sampling periods. For the spring 1981 deployment, it was decided to change the measurement format to acquire 17 min of wave data every 2 hr at a sampling rate of 1 Hz. The modified format still provided adequate definition of 3-sec and longer period waves while permitting a reduction in the interval between records from 3 to 2 hr, thus providing a more definitive record of the temporal changes in the wave climate.

6. It was assumed at the inception of the study that little of the wave energy propagating toward Saginaw Bay from Lake Huron would be transmitted across the shoal. There was, however, no observational basis for this assumption. If this assumption proved correct, Saginaw Bay could be treated as a closed basin for the purpose of hindcast modeling. This would eliminate the need to hindcast wave conditions in Lake Huron concurrent with those in Saginaw Bay and greatly simplify the problems involved in the modeling effort. Figures 4 and 5 show spectra obtained at locations 2 and 3, respectively, during the May 1981 storm. Examination of these spectra shows that very little of the wave energy in Lake Huron is propagating into Saginaw Bay. Indeed, the position of the peak of the spectrum obtained at location 2 implies the waves there to be almost totally locally generated under conditions of north and northeast winds, the most severe case for the assumption to be tested. Further examination of the time-history of significant height (measure of the total energy at the gage) results shown in Figure 6 reveals that initial growth rates at all three gage locations are uniform. Wave conditions at gage sites 3 and 2 become saturated while differences in the significant height results vary as much as 3.5 ft. Data in Figures 4, 5, and 6 clearly show that wave conditions found in Saginaw Bay will be caused by wave growth within the bay.

7. Comparison of spectra obtained at locations 1 and 2 allows calculation of the wave growth as functions of fetch and time. The fetch between these locations is about 16 statute miles.

# SAGINAW BAY

## WAVE DATA STATISTICS AND SPECTRAL PLOT

GAGE 6 YR 81 MO 5 DAY 10 LOCAL TIME 1640

$H_{M_0}$ (FT) 3.08 (M) 0.94 SPECTRAL PEAK (SEC) 4.19

$H_{1/100}$ (FT) 5.09 (M) 1.55 TOTAL ENERGY (FT²) 0.59 (M²) 0.05

RECORD LENGTH (SEC) 1024.0 NUMBER OF SAMPLES 1024

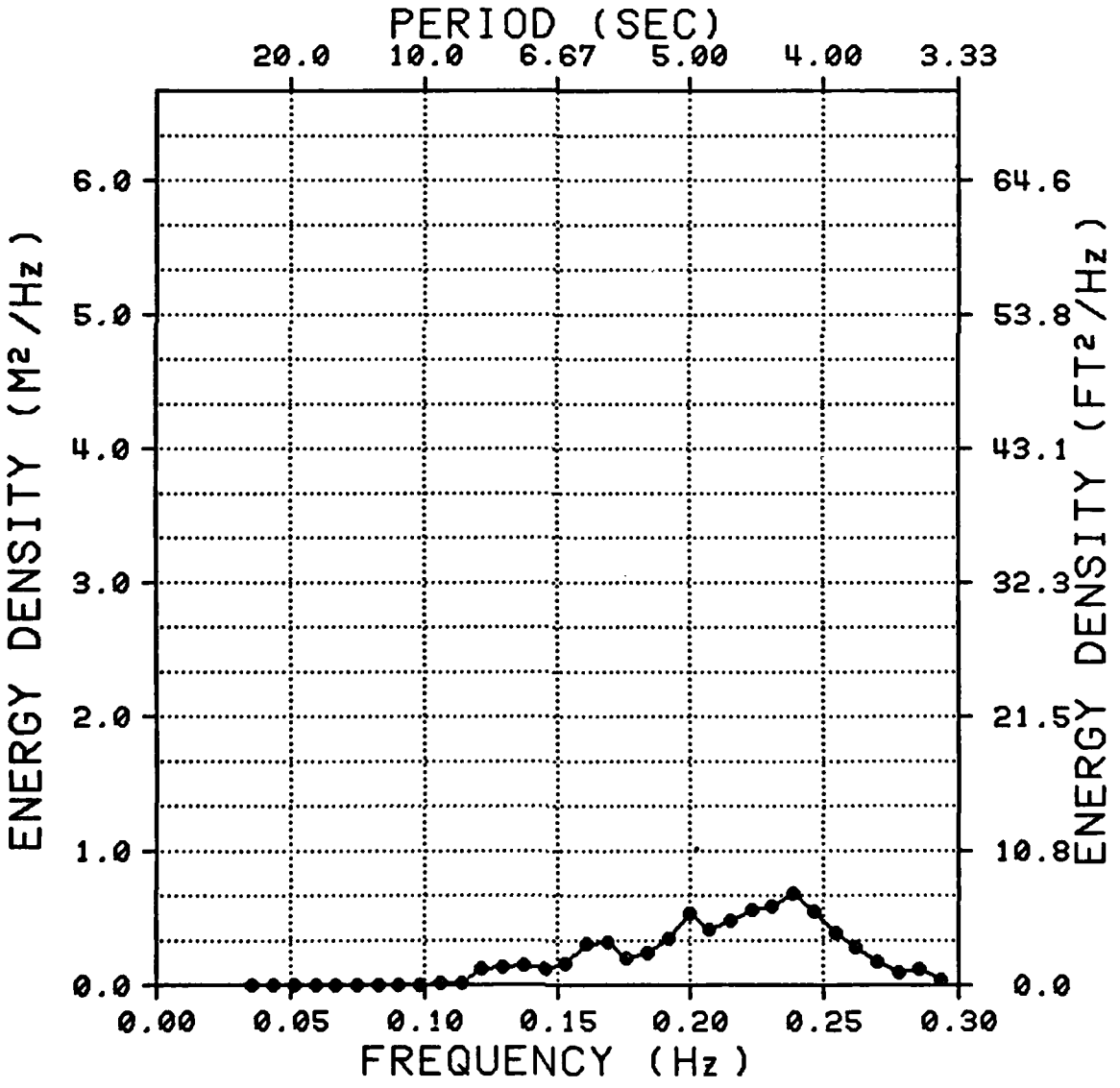


**Figure 4. Wave spectrum obtained at gage site 2 during May 1981 storm**

# SAGINAW BAY

## WAVE DATA STATISTICS AND SPECTRAL PLOT

GAGE 9 YR 81 MO 5 DAY 10 LOCAL TIME 1640

$H_{M_0}$ (FT) 6.23 (M) 1.90 SPECTRAL PEAK (SEC) 7.29

$H_{1/100}$ (FT) 9.78 (M) 2.98 TOTAL ENERGY (FT²) 2.42 (M²) 0.23

RECORD LENGTH (SEC) 1024.0 NUMBER OF SAMPLES 1024

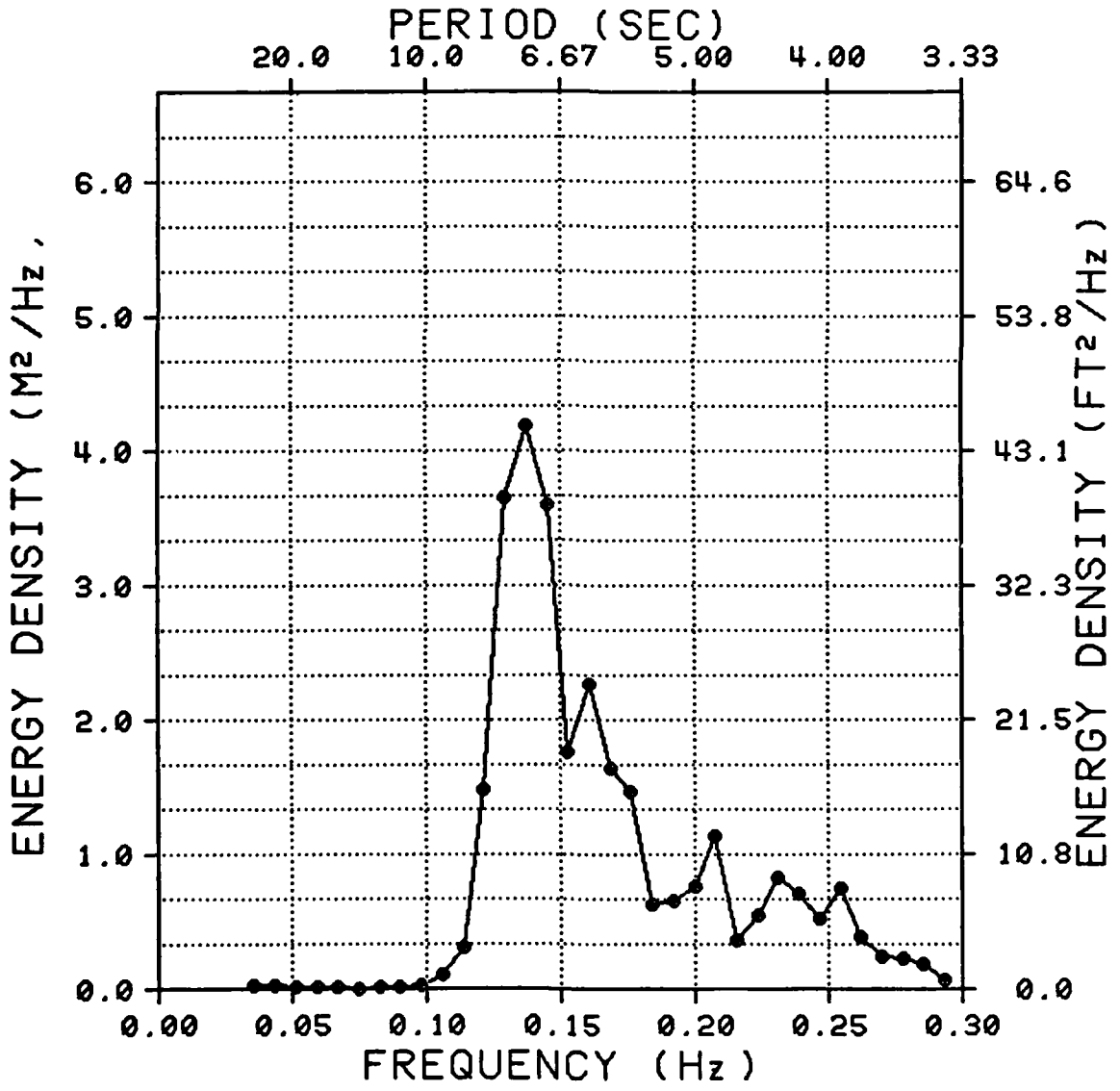


**Figure 5.** Wave spectrum obtained at gage site 3 during May 1981 storm

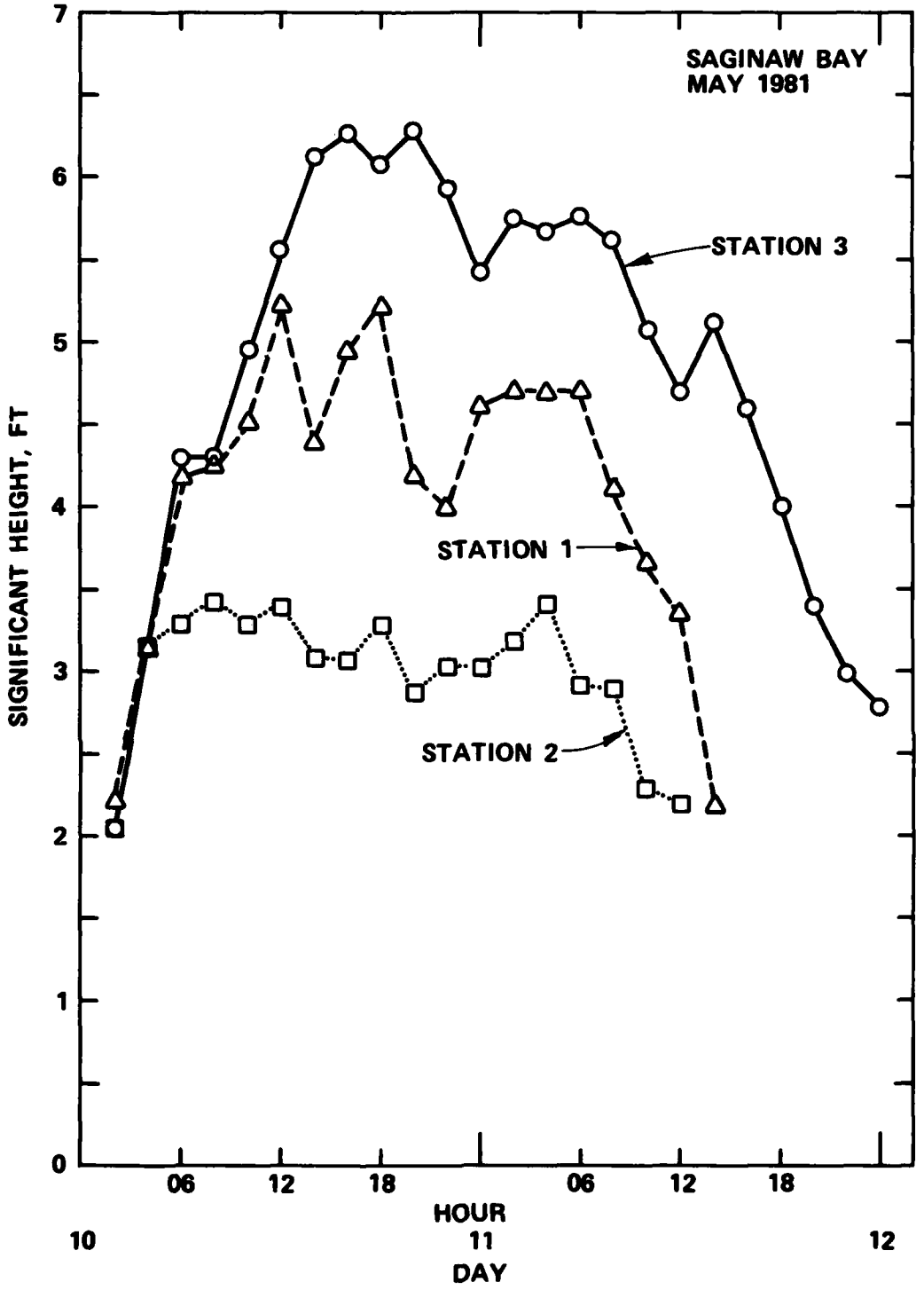


Figure 6. Significant wave heights at three gage stations during May 1981 storm

## PART III: WAVE-MEASUREMENT SYSTEM

8. The wave data acquisition system consisted of three completely submerged quadripod platforms, one at each of the locations shown in Figure 1. On each platform was mounted a commercially obtainable SEA DATA Model 635 wave gage. These are self-contained, pressure sensing instruments which record on standard Phillips type magnetic tape cassettes. This type of instrument was selected because the preferred locations are too far from shore to economically permit cabled sensors, and storms that tend to cause damage to the disposal facility are commonly accompanied by lightning which can interfere with or disable a telemetering type instrument. Moreover, Saginaw Bay is a popular boating and fishing area with the attendant boat traffic. Because of this traffic, it was felt that surface-following wave buoys would be vulnerable to vandalism or theft.

9. The quadripod platforms were positioned using electronic triangulation. It was originally thought that acoustic releases and beacons would be necessary for locating the platforms in order to service the gages. However, the electronic positioning proved to be repeatable to within about 10 m of the positions of the platforms, thereby eliminating the need for the releases and beacons. Small witness buoys were used to mark the location of the platforms but these were expendable and used more to assist the boat operator and divers in station keeping during servicing than as a required locating aid.

10. The data tapes retrieved from the gages were returned to WES for processing. The wave spectra were computed via a discrete Fast Fourier Transform and corrected for depth attenuation according to linear wave theory as a function of frequency. The pressure response factor P is computed as

$$P = \frac{\cosh kh}{\cosh kD} \tag{1}$$

where

k = local wave number*

h = local water depth

D = height of the wave sensor above the bottom

---

* For convenience, symbols are defined in the Notation (Appendix B).

The spectral energy density of the sea surface is thus related to the pressure spectrum by the equation

$$E_s(f) = \left(\frac{\cosh kh}{\cosh kD}\right)^2 E_p(f) \tag{2}$$

where

subscripts s, p = surface and pressure spectra, respectively.

The significant wave height $H_{m_0}$ is computed as

$$H_{m_0} = 4\left[\int_{1/T}^{\frac{1}{2\Delta t}} E_s(f)df\right]^{1/2} \tag{3}$$

where

$\Delta t$ = sampling interval, sec

T = length of a wave record, sec

For the data obtained at Saginaw Bay, T = 1,024 sec; for the data obtained in years 1979 and 1980, $\Delta t$ = 0.5 sec; for 1981, $\Delta t$ = 1 sec. The sampling interval was increased for two reasons. First, it was observed in the wave data obtained during 1979 and 1980 that there was little energy in the frequencies above about 0.3 Hz; second, the wave climate at each of the locations could change markedly in a 3-hr period which was the length of time between wave records acquired during 1979 and 1980. Thus it was decided to increase the sample interval from 0.5 to 1.0 sec and decrease the interval between sample records from 3 to 2 hr.

## PART IV: THEORY OF THE SHALLOW-WATER WAVE MODEL

11. The predictions of shallow-water wave characteristics have become a focal point of research activities across the world. Because construction, shipping, and dredging operation costs have drastically increased over the years, coastal engineers have been faced with more accurately defining the shallow-water wave climate. A better understanding of shallow-water wave growth and transformation mechanisms is slowly evolving through controlled wave-measuring programs such as ARSLOE (Vincent and Lichy 1981). However, not all of the questions have been answered, and it will take some time before all shallow-water wave transformation mechanisms are quantified. In light of this, the shallow-water wave modeling technique (SWWM) employed in this study adopts "state-of-the-art" mechanisms currently available. The main intent in the development of the SWWM is to describe the physical processes as accurately as possible while simplifying the computational procedures to a degree where shallow-water wave hindcasting is economically feasible.

12. Hasselmann et al. (1976) introduced a parametric model of wind-wave generation relating the rate of energy growth to nondimensional characteristics of the wind field. The energy growth (in space or time) is governed by a self-similar process and verified through extensive prototype data (Hasselmann et al. 1973, 1976). In these studies, the dominant energy input to the forward face of the spectrum is related to convergence of energy flux due to nonlinear, resonant wave-wave interactions (Figure 7) of the form described by Hasselmann (1962). Studies by Mitsuyasu (1968, 1969) and Kitaigordskii (1962) also displayed similar results. Although these formulations were developed for deepwater wave conditions, they are used in the SWWM because the only formulation of the nonlinear transfers is based specifically on JONSWAP type wave spectra.

13. The rate of wave growth under ideal conditions of fetch limitations or duration limitation and a stationary wind field can be computed (Hasselmann et al. 1976). For growth along a fetch the solution is

$$E_o = 1.6 \times 10^{-7} U^2 \frac{F}{g} \tag{4}$$

and for growth through time, it becomes

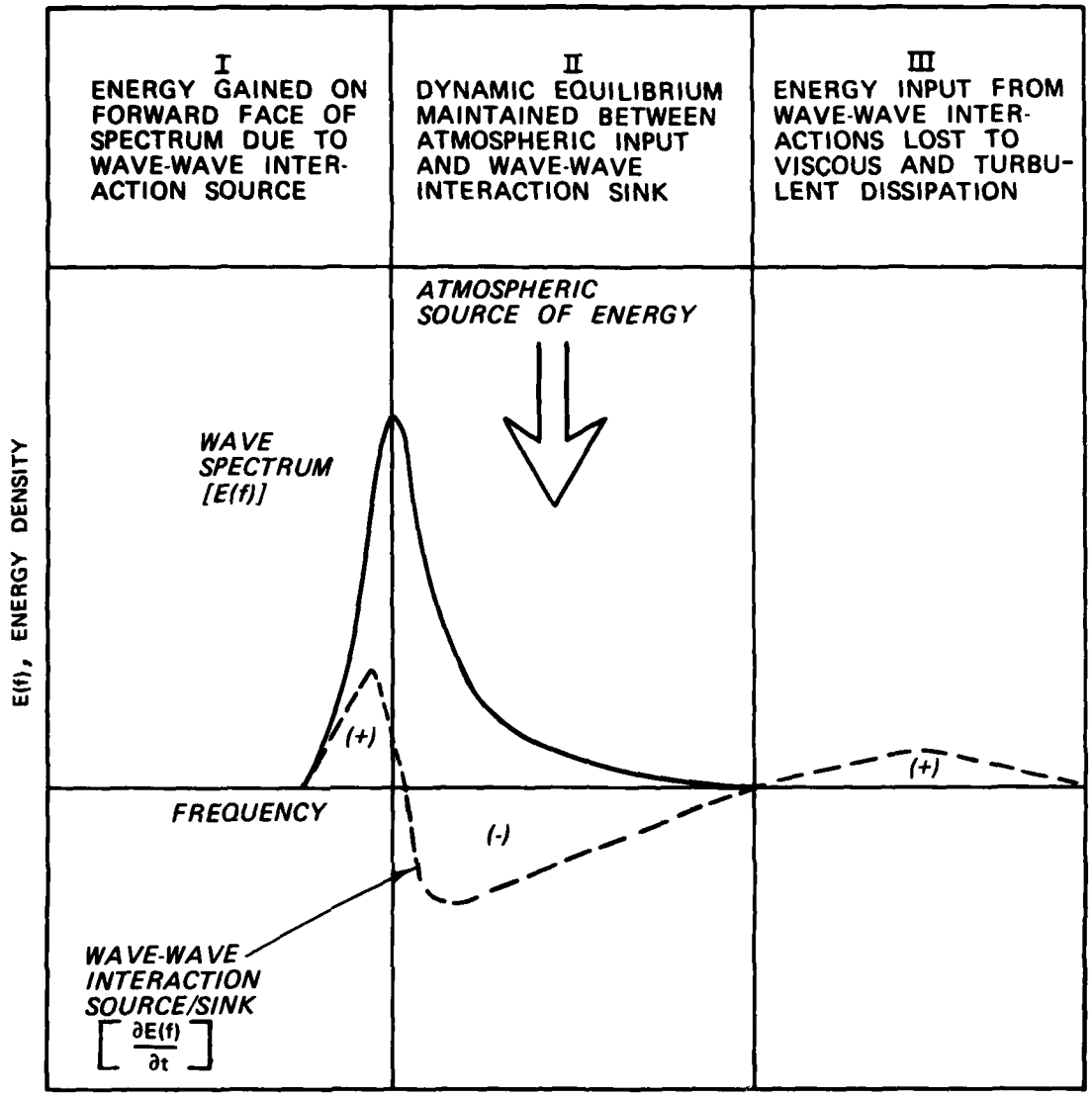


Figure 7. Schematic representation of the nonlinear wave-wave interactions

$$E_o = 4.3 \times 10^{-10} U^{18/7} g^{-4/7} t^{10/7} \quad (5)$$

where $E_o$ is the total energy resulting from a wind speed $U$ (assumed to be overwater wind conditions adjusted to 33-ft elevation), blowing over a given fetch length $F$. The gravitational acceleration is denoted by $g$; $t$ is the time since the wind began to blow.

14. Two additional pieces of information are required to quantify the distribution of $E_o$ given in the form of an energy density spectrum. The nondimensional peak frequency, $\tilde{f}_m$, and the Phillips' equilibrium

constant $\alpha$ (Phillips 1957) are shown in Figures 8 and 9. These parameters are written as

$$\alpha = 0.076\hat{X}^{-0.22} \tag{6}$$

and

$$\hat{f}_m = 3.5\hat{X}^{-0.33} \tag{7}$$

where $\hat{X}$ is the nondimensional fetch length

$$\hat{X} = \frac{gF}{U^2} \tag{8}$$

15. The selection of fetch (Equation 4) or duration limited conditions (Equation 5) is determined from the following:

$$t_{min} = 5.37 \times 10^2 \left(\frac{U}{g}\right)\left(\frac{gT_s}{U^2}\right)^{7/3} \tag{9}$$

where $t_{min}$ is the minimum duration condition and $T_s$ is the significant wave period (U. S. Army CERC 1981b) given by:

$$T_s = 7.54 \frac{U}{g} \tanh\left(0.833 \frac{g\bar{h}}{U}\right) \tanh\left\{\frac{0.0379\left(\frac{gF}{U^2}\right)^{1/3}}{\tanh\left[0.833\left(\frac{g\bar{h}}{U^2}\right)^{3/8}\right]}\right\} \tag{10}$$

where $\bar{h}$ is the mean water depth along $F$.

16. If $t_{min}$ is less than 3 hr (duration of each input wind condition), then Equation 5 will be used to compute the total energy; otherwise Equation 4 will be employed.

17. The parameterization of the wave growth is restricted such that when the nondimensional peak frequency attains a value of 0.13 or less, a fully developed sea state is achieved and wave growth is halted. Over long fetch lengths and low wind speeds, this condition can occur with some degree of regularity. Thus Equations 4-8 are then redefined by

$$Q = K \sum_{i=1}^{10} \zeta_i \tag{11}$$

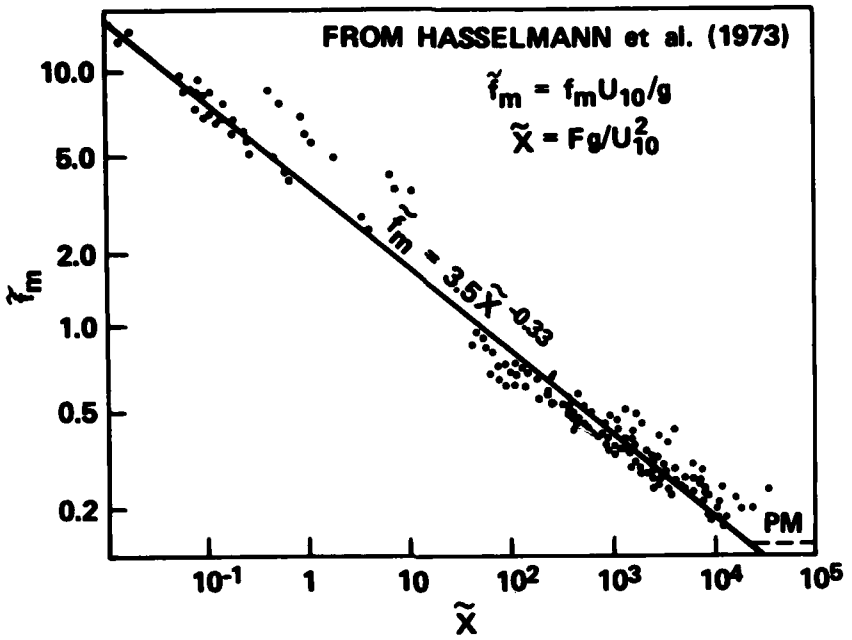


Figure 8. Nondimensional peak frequency $f_m$ as a function of nondimensional fetch length $\tilde{X}$

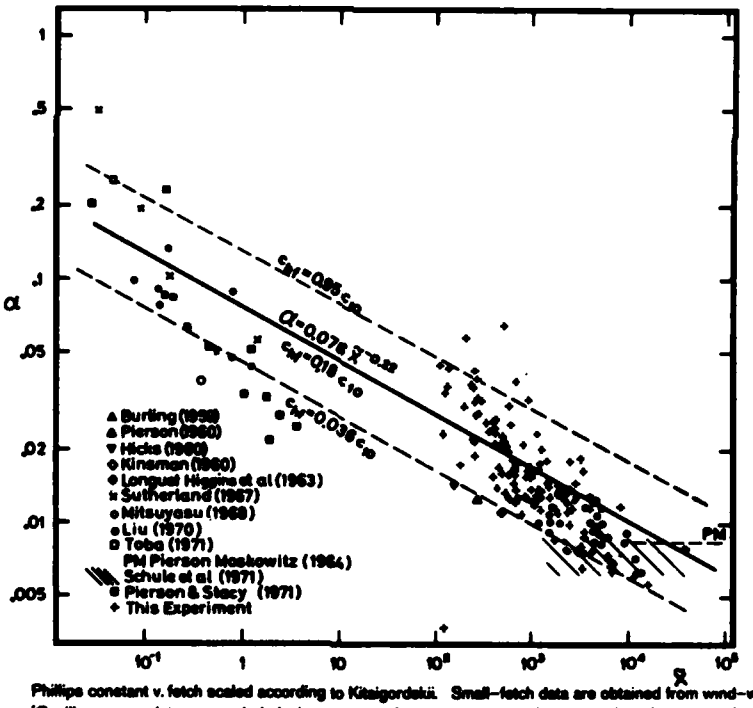


Phillips constant v. fetch scaled according to Kitaigorodskii. Small-fetch data are obtained from wind-wave tanks. (Capillary-wave data was excluded where possible.) Measurements by Sutherland (1967) and Toba (1971) were taken from W.J. Pierson and R.A. Stacy (1973)

Figure 9. Phillips' equilibrium constant $\alpha$, as a function of nondimensional fetch length $\tilde{X}$, from Hasselman et al. (1973)

where $K$ is defined as the nonvarying parameters (and constants), $Q$ is defined as the dependent parameters, and $\zeta_i$ is recognized as the independent parameters ($F$ and $\tilde{X}$) found in Equations 4-8. The parameter $i$ is the increment counter. After each discrete fetch length $F_i$, the nondimensional peak frequency is evaluated to determine if $\tilde{f}_m \leq 0.13$. If this occurs wave growth is terminated, and wave decay is initiated for the remainder of the fetch length. Wave decay is parameterized following the work conducted by Bretschneider (1952) and Mitsuyasu and Kimura (1965) for $f_m$ the peak frequency (where $f_m = \tilde{f}_m g/U$) while the total energy decay rate follows that described by Jensen (in preparation).

18. Wave conditions generated in Saginaw Bay also must consider dispersion effects resulting from finite water depth conditions. When the water depths vary from $F_i$ to $F_{i+1}$, the conservative transformation mechanisms of shoaling and refraction must be considered. Wave shoaling is determined from the evaluation of group speed determined by linear theory. Wave refraction is neglected under the assumption that: the bottom topography is assumed to be straight and parallel for every fetch length. Considering the water depths in Saginaw Bay and peak wave periods ($T_p = 1/f_m$) in the range of 2 to 8 sec, wave-refraction effects (and subsequent "errors") would be on the order of 2 to 25 percent as shown by Figure 10, designated by the crosshatched area. This is assuming that at most, the angle between the wave crest and bottom contour is 30 deg. The initial direction of wave propagation is limited to 18 angle classes at 10-deg increments (because of the wind data employed in this study); thus the accuracy in the resultant refracted wave condition, by similarity, also would be constrained to the 18 angle classes.

19. Finite water depth conditions also lead to bottom dissipation effects on the growing seas. Energy losses associated with bottom friction are empirically modeled using the following sets of equations developed by Bretschneider and Reid (1954):

$$E = E_1 \left( \frac{ff\ E_1\ \phi_f\ \Delta F_i\ f_m^4}{K_s} \right)^{-1} \tag{12}$$

where

$E$ = final total energy at $F_i$

$E_1$ = original total energy at $F_{i-1}$

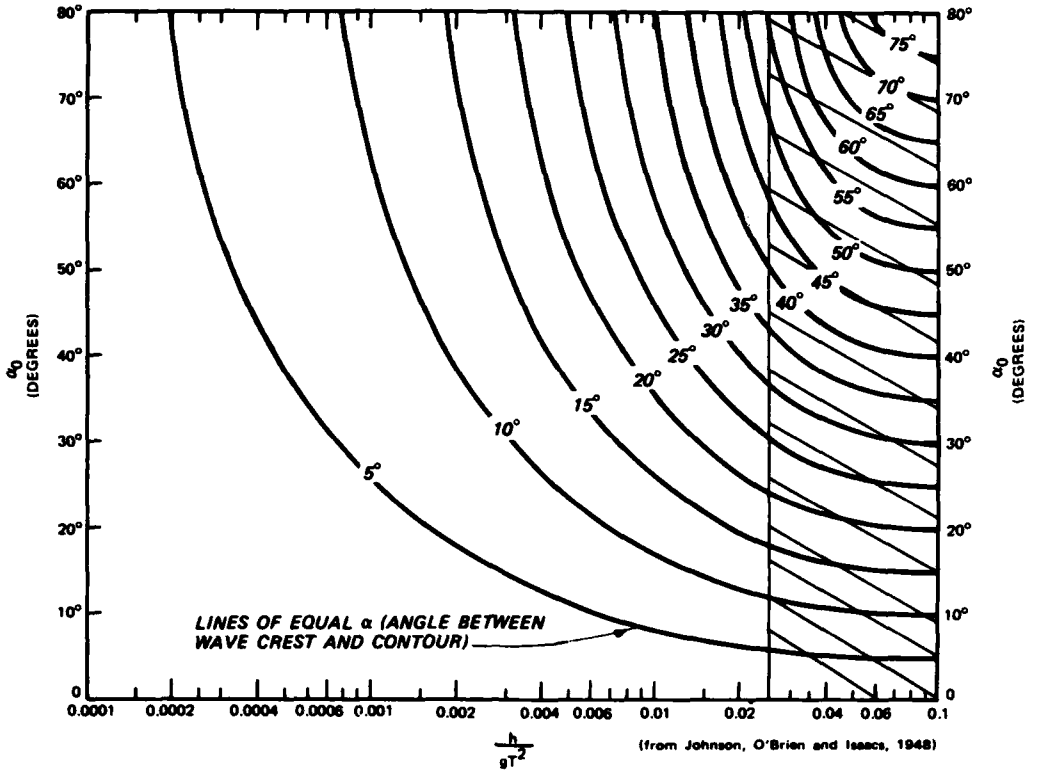


Figure 10. Changes in wave direction due to refraction on slopes with straight and parallel depth contours

ff = nondimensional friction factor (set for Saginaw Bay at 0.001)

$\Delta F_i$ = distance of wave travel within the discrete fetch length

$$K_s = \tanh (k_i h_i) \left[ 1 + \frac{2k_i h_i}{\sinh (2k_i h_i)} \right]^{-1/2} \tag{13}$$

and

$$\phi_f = \frac{64\pi^3}{3g^2} \left[ \frac{K_s}{\sinh (2k_i h_i)} \right]^3 \tag{14}$$

where

$k_i$ = wave number ($k_i = \frac{2\pi}{L_i}$)

$L_i$ = wavelength evaluated for $f_m$

$h_i$ = water depth at $F_i$

20. The second theoretical aspect of SWWM deals primarily with the distribution of the total energy ($E_o$) in the form of a one-dimensional discrete frequency spectrum $E(f_j)$. Through the use of similarity principles, Kitaigordskii, Krasitskii, and Zaslavaskii (1975) extended Phillips' deepwater hypothesis (Phillips 1958) of the equilibrium range in the spectrum of wind-generated surface waves to finite depth conditions. The spectral form is defined by

$$E(f_j) = \alpha g^2 (2\pi)^{-4} f_j^{-5} \Phi(\omega_h) \qquad f_j \geq f_m \tag{15}$$

where $E(f_j)$ is the energy density at each discrete frequency band, $f_j$, and $\Phi(\omega_h)$ is a nondimensional function dependent on $\omega_h$ given by

$$\omega_h = 2\pi f_j (h/g)^{1/2} \tag{16}$$

The function $\Phi(\omega_h)$ varies from 1.0 in deep water to 0.0 when $h = 0.0$, as shown by Figure 11. When $\omega_h$ is less than 1.0, $\Phi(\omega_h)$ can be approximated by:

$$\Phi(\omega_h) \cong \frac{1}{2} \omega_h^2 \tag{17}$$

and therefore,

$$E(f_j) = \frac{1}{2} \alpha g h (2\pi)^{-2} f_j^{-3} \qquad f_j \geq f_m \tag{18}$$

or, the spectral shape changes from $f^{-5}$ to $f^{-3}$ in the tail of the energy

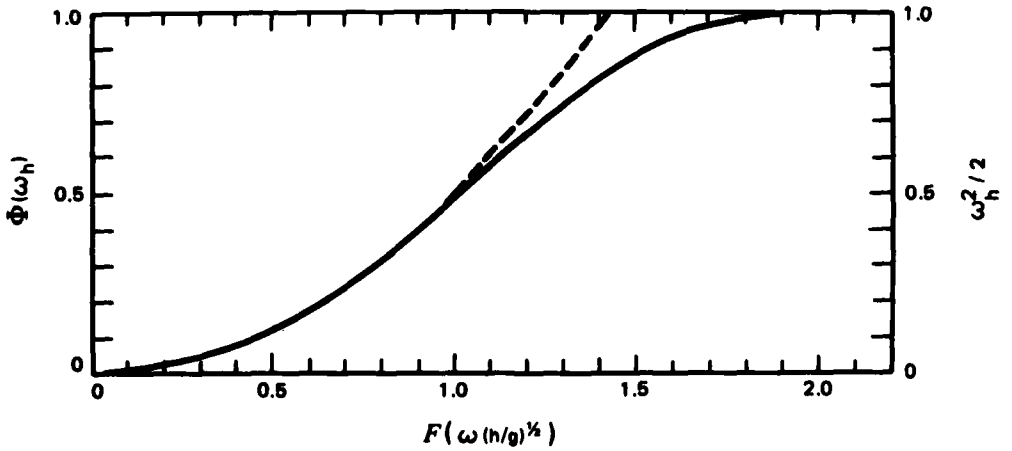


Figure 11. The universal dimensionless function $\Phi$ (solid curve) and the function $\delta_h^2/2$ (dashed curve), from Kitaigordskii, Krasitskii, and Zaslavaskii (1975)

density spectrum, and more importantly, becomes a function of the water depth.

21. The forward face of the spectrum is assumed to be represented by:

$$E(f_j) = \alpha g^2 (2\pi)^{-4} f_m^{-5} \exp\left[1 - \left(\frac{f_m}{f}\right)^4\right] \Phi'(\omega_h) \qquad f_j < f_m \qquad (19)$$

where $\Phi'(\omega_h)$ is evaluated from the $\omega_h$ defined at $f_m$. Field and laboratory data by Goda (1974), Thornton (1977), Ou (1980), Iwata (1980), and Vincent (1981) support the form given by Equation 18. The verification of Equation 19 can be found in Vincent* and is supported by this study.

22. The parametric representation of wave growth assumes a dynamic balance between atmospheric sources and transfers of energy resulting from wave-wave interactions (Figure 6). This parameterization was based on deep-water wave conditions, Hasselmann et al. (1976). During this study, it was determined that over moderately short fetch lengths (10 to 20 n.m.), this deep-water growth rate expression (Equations 4 and 5) consistently underpredicted the total energy found in the measured data. The only theoretically consistent location to add the energy would be on the forward face of the spectrum (Figure 12). The function, $E(f,h)_{THEORY}$ is the saturated spectrum based on Equations 15 and 19, and $E(f,h)_{WEIGHTED}$ is the spectrum based on $E_o$ after wave growth. This process also shifts $f_m$ to a lower frequency which has been noticed in field data (Vincent**). As the fetch length increases, the relative amount of added energy decreases, where eventually no additional energy is incorporated into the resulting spectrum.

23. It has been shown that the water depth greatly influences the spectral shape and in so doing will influence the maximum wave condition. The parametric formulation follows the work conducted by Vincent (1981). The depth limiting maximum wave condition is given by,

$$H_m = 4\sqrt{\int_{f_c}^{\infty} E_m(f)\, df} \qquad (20)$$

---

* Personal communication, C. L. Vincent (1982a), U. S. Army CERC, Fort Belvoir, Va.

** Personal communication, C. L. Vincent (1982b), U. S. Army CERC, Fort Belvoir, Va.

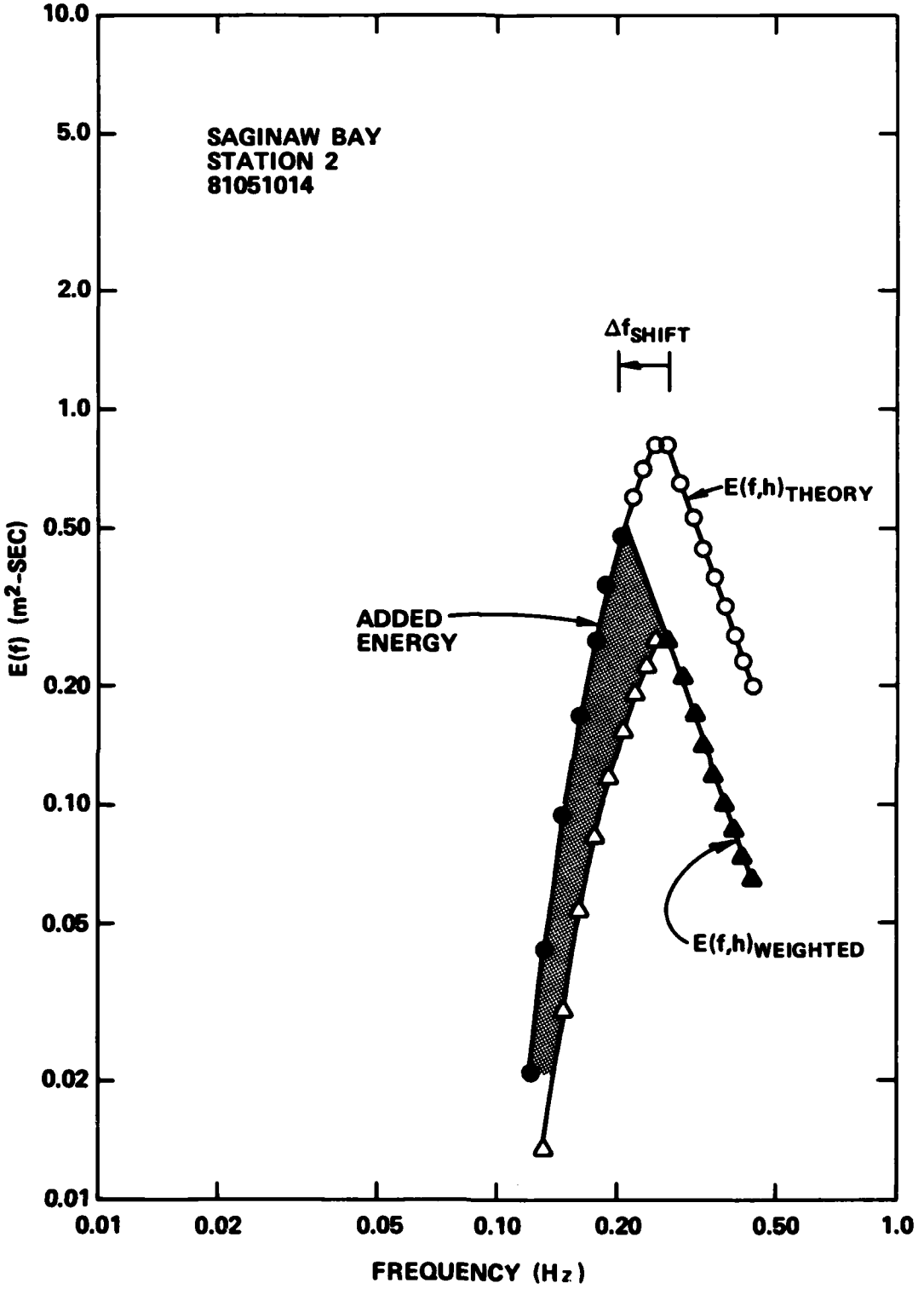


Figure 12. Construction of the final energy density spectrum (solid symbols) caused by shallow-water wave generation

where

$H_m$ = the maximum wave condition

$f_c$ = the lower frequency bounding the total energy (equal to 0.9 $f_m$)

$E_m(f)$ = is defined from Equation 12

Integrating Equation 20 the absolute limit on the wave condition at a particular water depth is obtained, where

$$H_m = \frac{(\alpha g h)^{1/2}}{\pi f_c} \tag{21}$$

24. In summary, the physical process governing wave generation and transformations has been theoretically determined using available, state-of-the-art techniques. It must be emphasized that not all shallow-water transformation processes have (or can be) measured to determine their relative effect on the total energy, spectral shape, and peak frequency. Therefore the development of the SWWM as employed in this study attempts to model the physics of the problem in a general sense while maximizing computational efficiency.

## PART V: COMPARISONS

25. In all wave hindcasting studies, comparisons to gage measurements are a necessary element in the development of a wave model. The initial calibration test was conducted on a data set that contained the largest wave conditions measured during the wave gaging portion of this study.

26. The wave gages were deployed in April 1981 shortly after the bay became ice-free. Early on 10 May 1981, winds began to increase and by noon were steady at 25 to 30 mph from a direction of about 40 deg east of north. The winds held a remarkably constant speed and direction for about a day and a half before beginning to diminish. The predominant direction coincided with the axis of the bay and alignment of the gage array, the most favorable condition for generation of the largest waves and for studying changes in the wave climate.

27. Because of the constancy in the wind speed and direction during the period 10-12 May 1981, any variation in the wave climate would be a function only of the wind speed. Figure 13 shows the wind data obtained at the Saginaw Projects Office during this period of time. The anemometer elevation was about 60 ft and located about 3 miles south of the disposal facility.

28. Results of the comparisons for gage sites 1 and 2 are shown in Figures 14-17 where $H_{m_0}$ is the significant wave height and $T_p$ is the peak period defined as:

$$H_{m_0} = 4\sqrt{\int_0^\infty E(f)\ df} \tag{22}$$

$$T_p = \frac{1.0}{f_m} \tag{23}$$

There is a slight phase difference between the measured and hindcast data sets. This is due to the SWWM assumption that wave conditions are generated instantaneously, i.e., there is no time-dependency associated with the effects of wave propagation on the wave climate. The small-scale temporal fluctuations in the measured data cannot be simulated in the SWWM because of the assumption of uniform wind conditions.

29. Energy density comparisons are also made between the measured and hindcast data. It is helpful to recognize that a spectral representation of

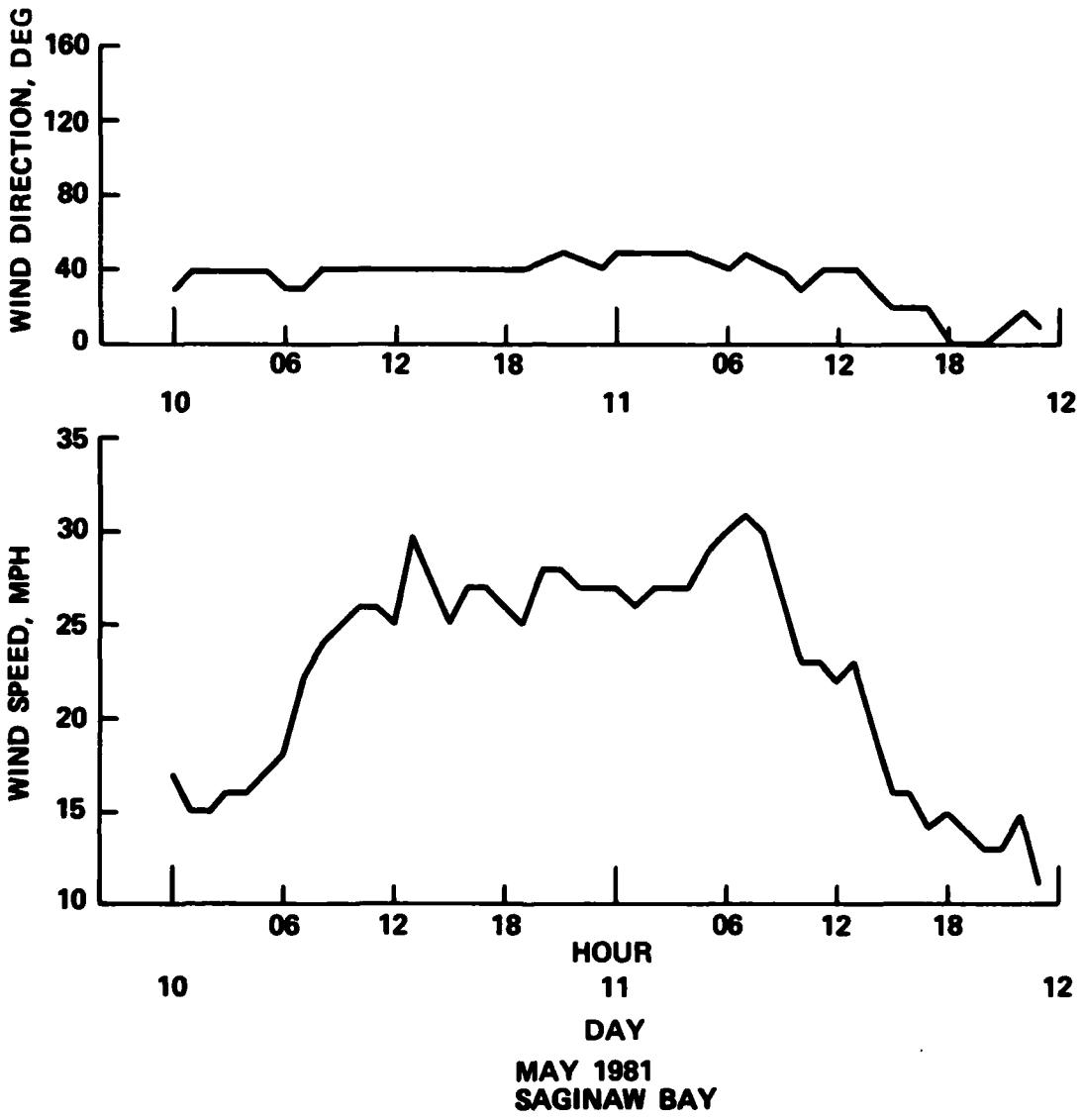


Figure 13. Wind data used for calibration test

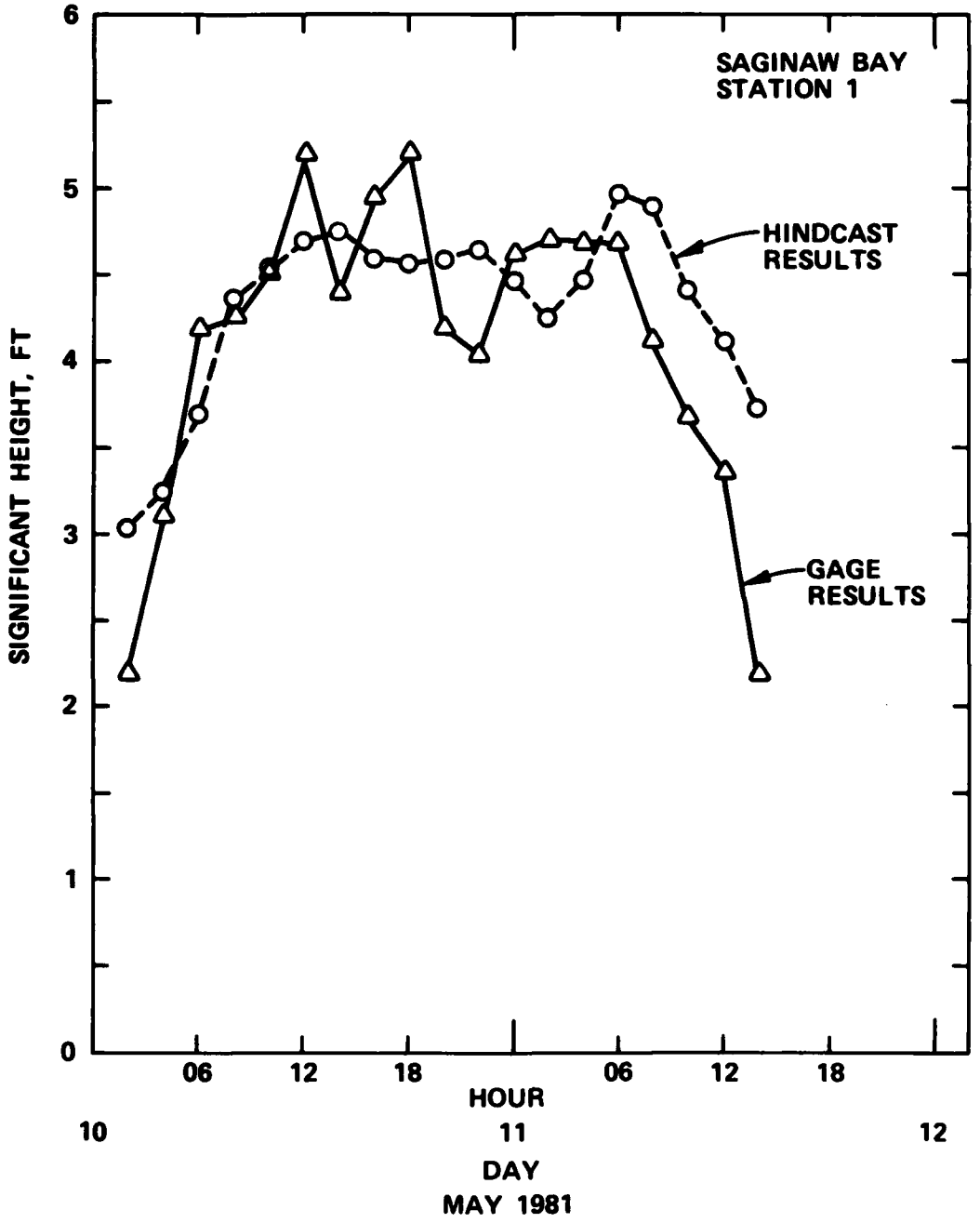


Figure 14. Comparison between measured and hindcast significant wave-height data for Station 1

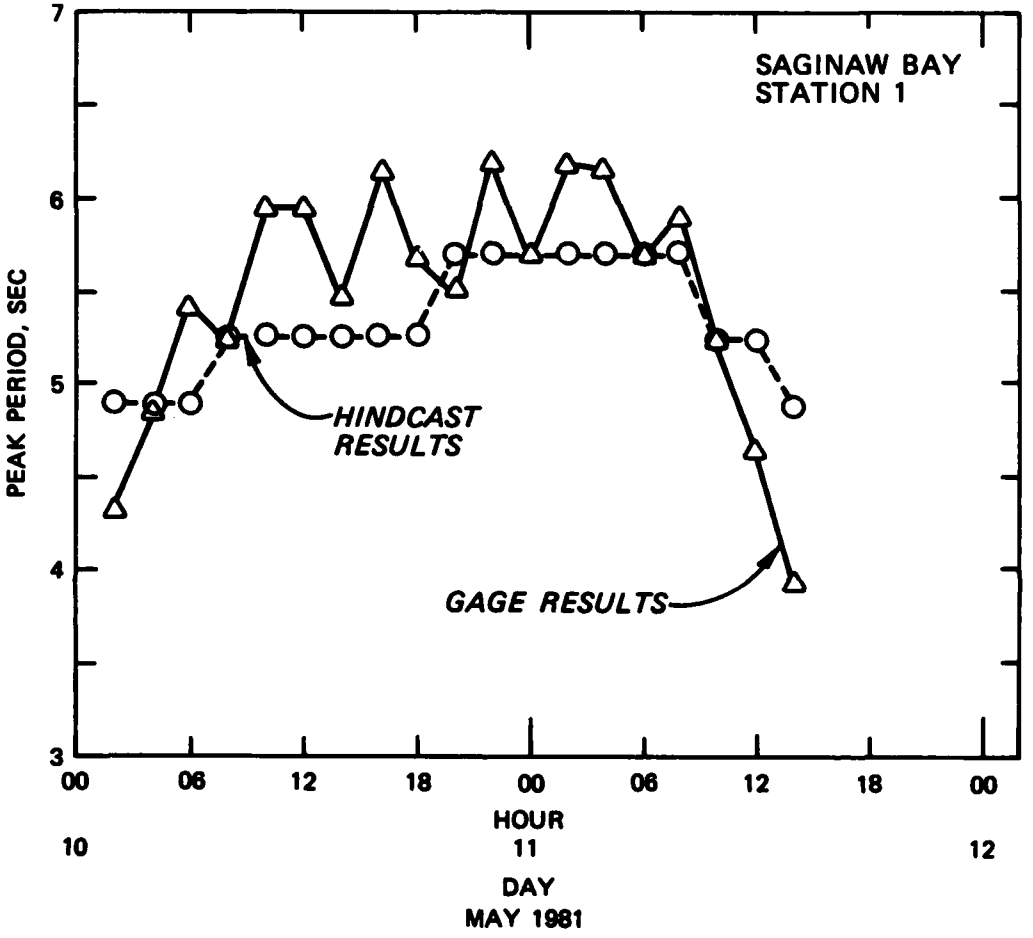


Figure 15. Comparison between measured and hindcast peak wave period data for Station 1

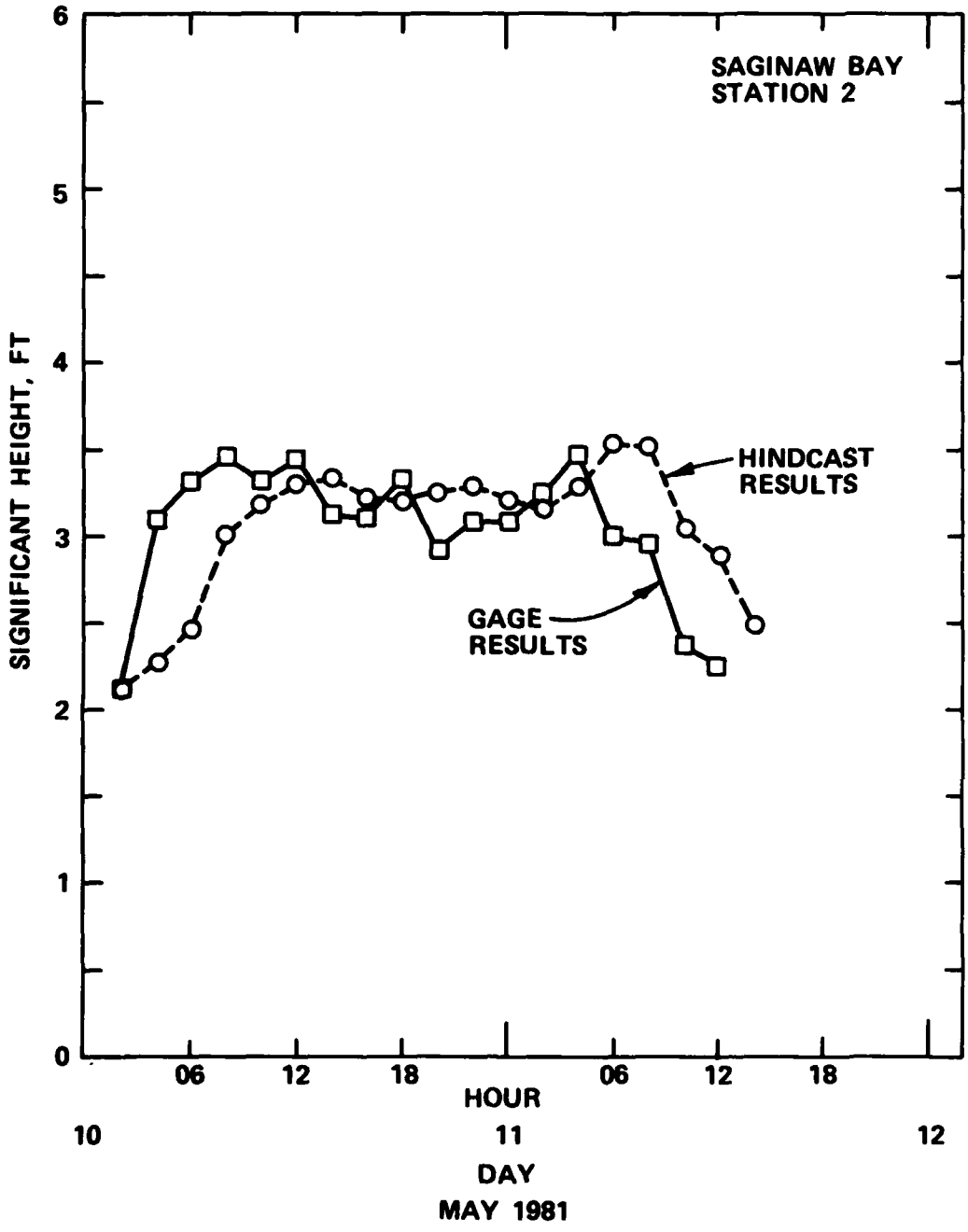


Figure 16. Comparison between measured and hindcast significant wave-height data for Station 2

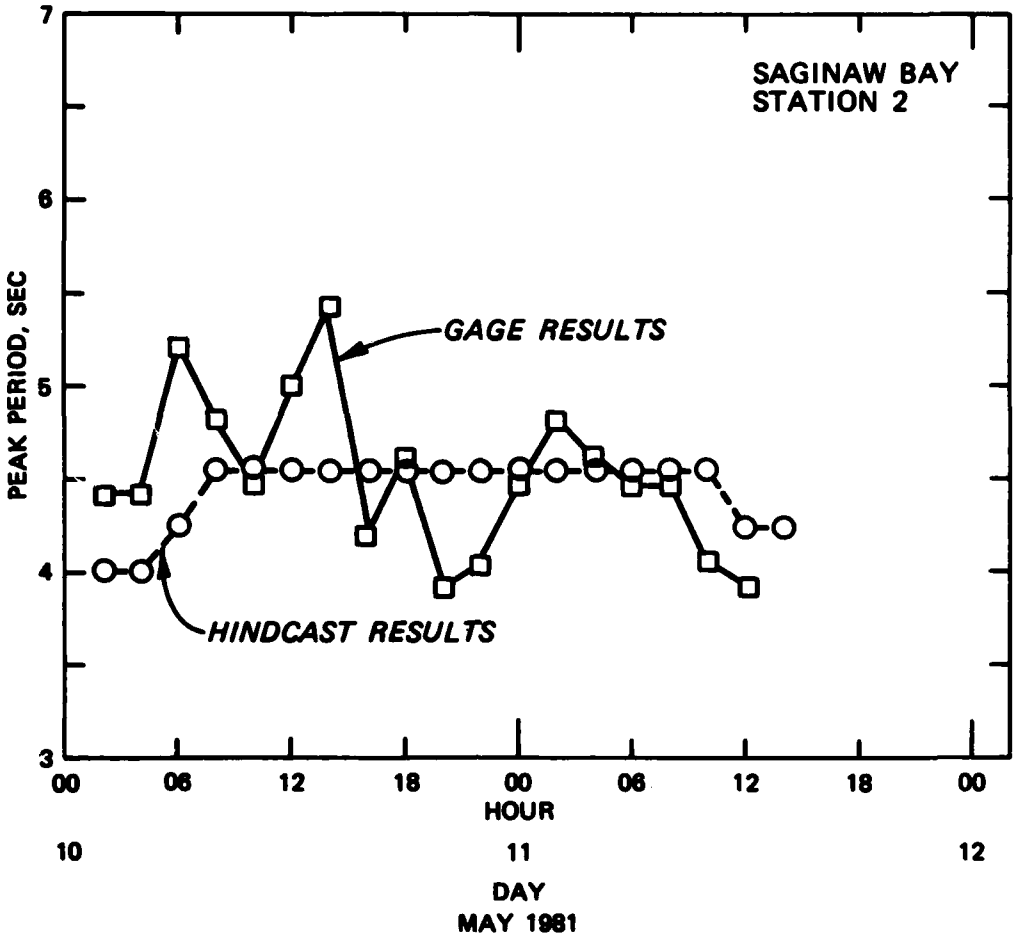


Figure 17. Comparison between measured and hindcast peak wave period data for Station 2

the wave phenomena is an estimate of the actual wave conditions existing at a specific point in space and time. To illustrate this, all measured wave spectra are plotted with an accompanying 90 percent CHI-squared distribution confidence band. Although numerous comparisons were performed, a limited number of Station 1 results are presented. The five energy density spectral plots shown in Figures 18-22 represent four phases in the 10-12 May 1981 storm; Figures 18 and 19 illustrate the initial growth phase, Figure 20 illustrates the initial decay phase, Figure 21 illustrates the secondary growth phase, and Figure 22 illustrates the final decay stage. The SWWM spectral results are adjusted in time to compensate for the lag associated with the wave propagation. The adjustment varies from 2 to 4 hr depending on propagation time.

30. The energy plots (E(f) versus f) are plotted in a nondimensional frequency domain defined by $f/f_m$ where $f_m$ is the frequency at the spectral

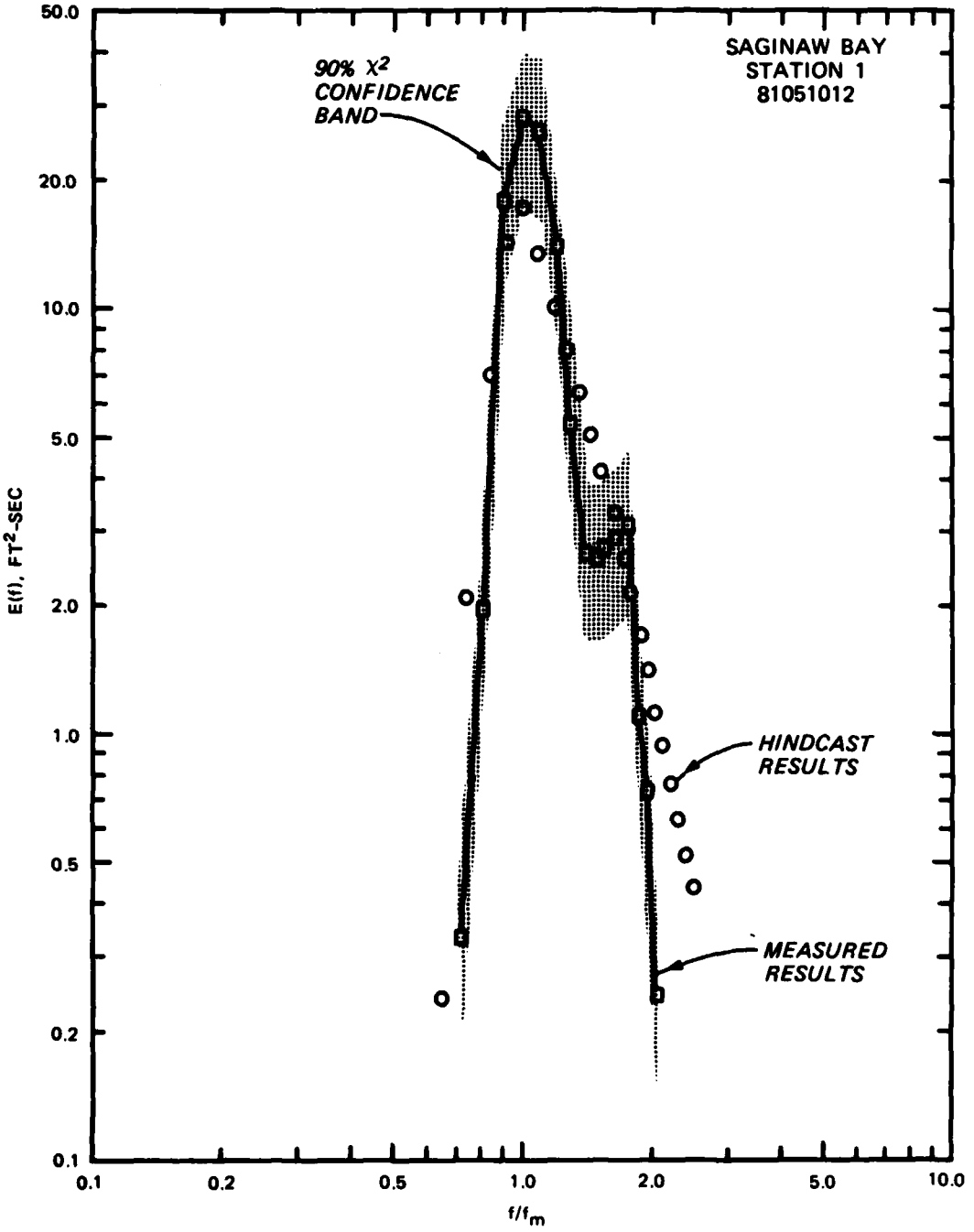


**Figure 18. Comparison between measured and hindcast wave spectra, Station 1, 1200 hours, 10 May 1981**

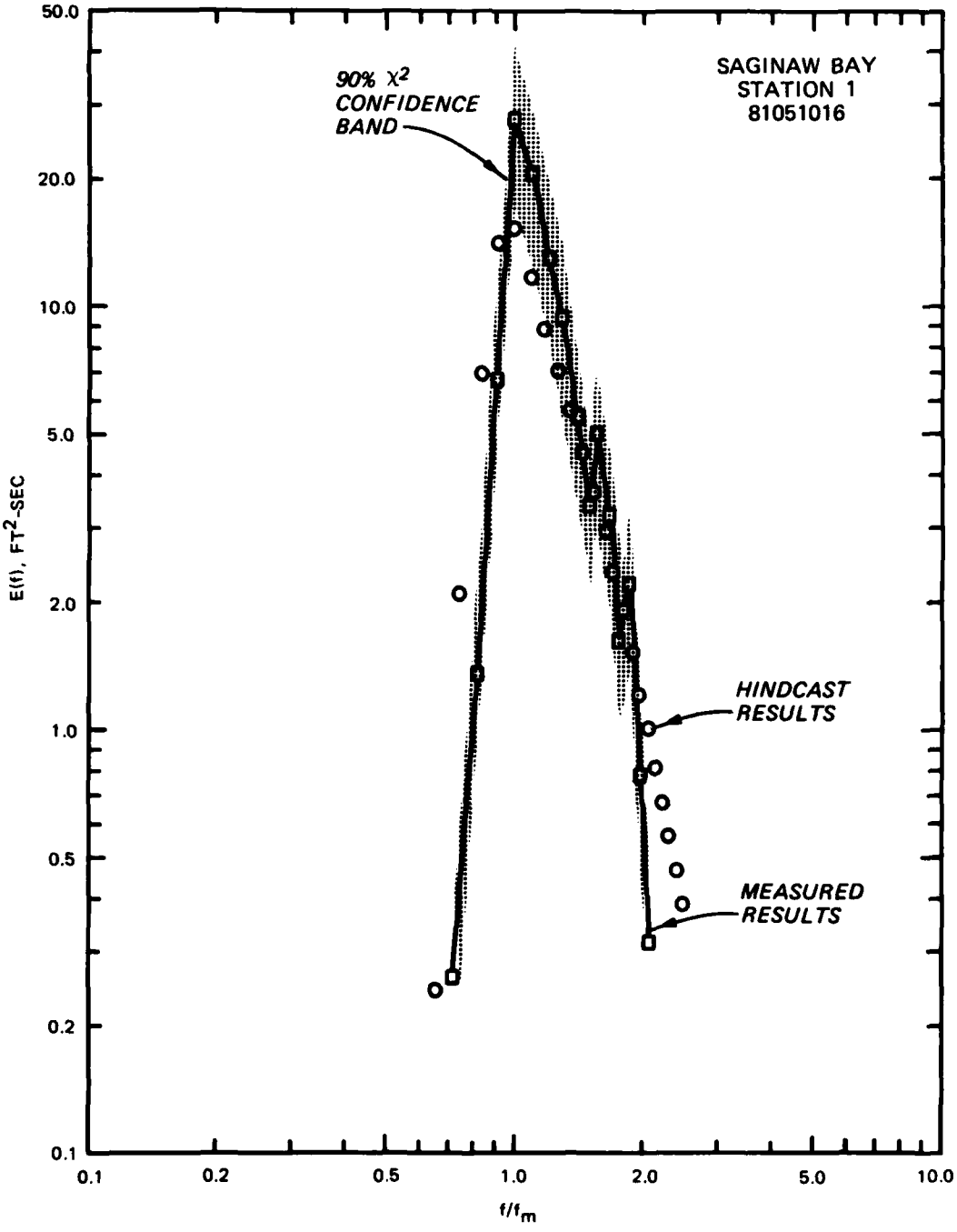


Figure 19. Comparison between measured and hindcast wave spectra, Station 1, 1600 hours, 10 May 1981

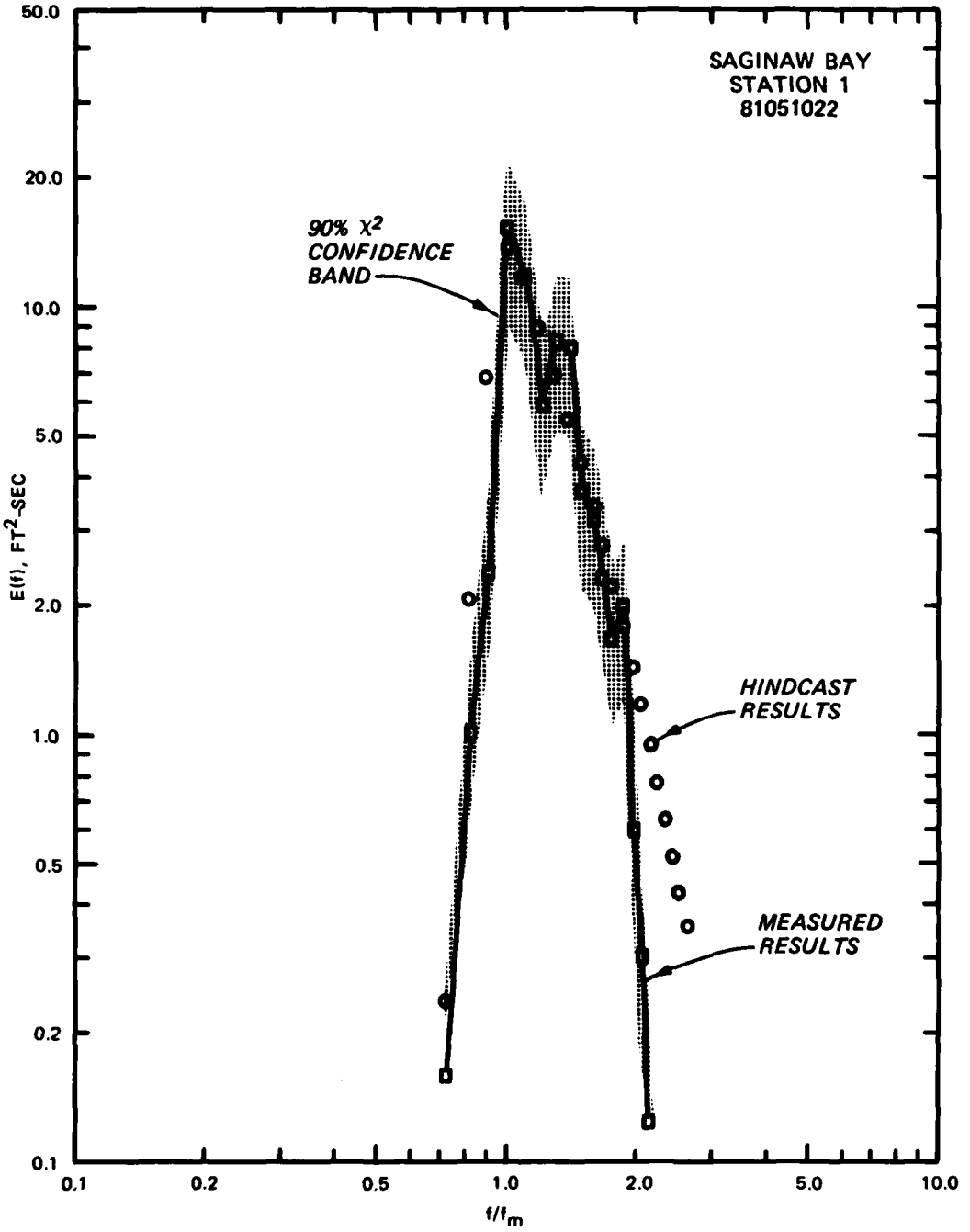


Figure 20. Comparison between measured and hindcast wave spectra, Station 1, 2200 hours, 10 May 1981

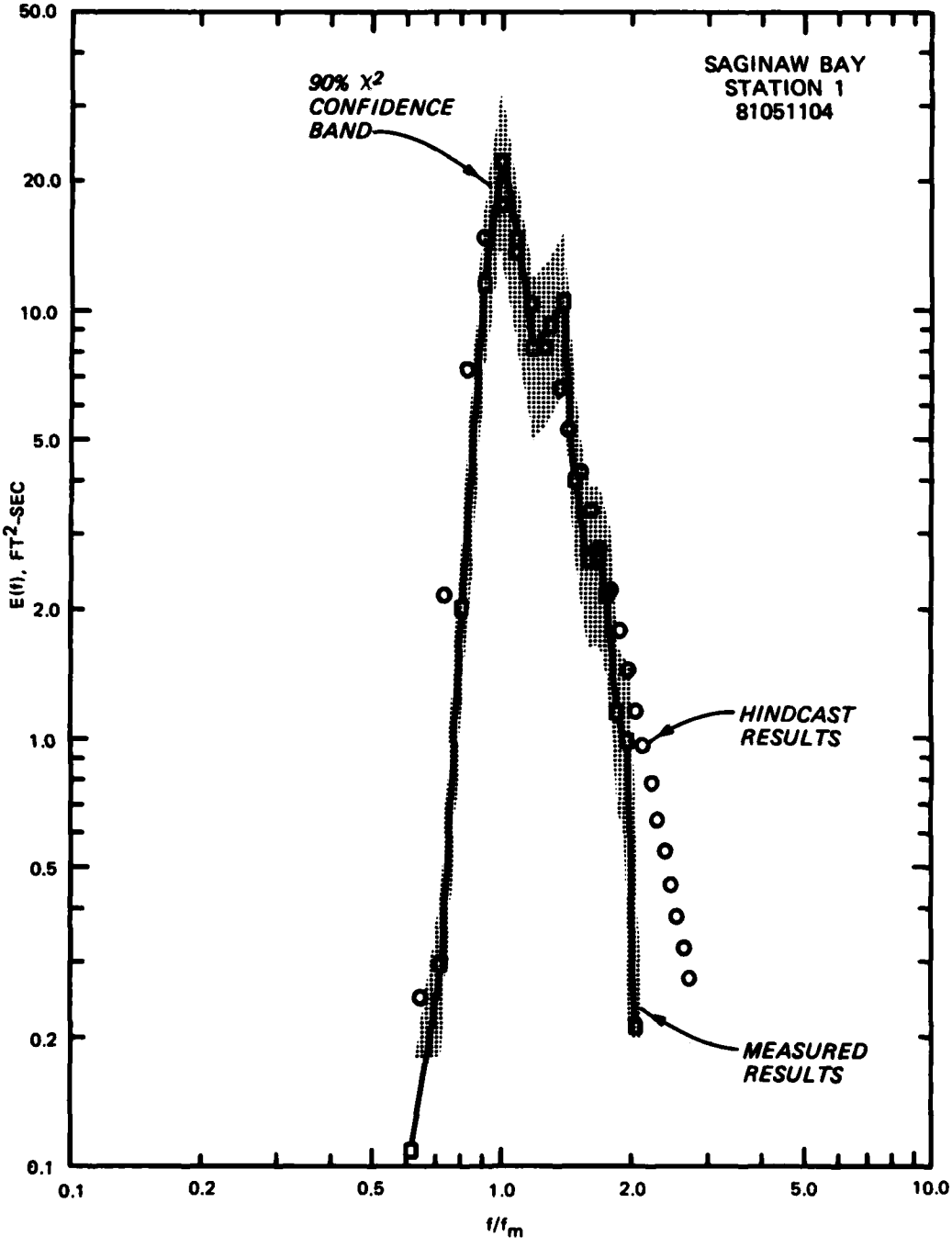


Figure 21. Comparison between measured and hindcast wave spectra, Station 1, 0400 hours, 11 May 1981

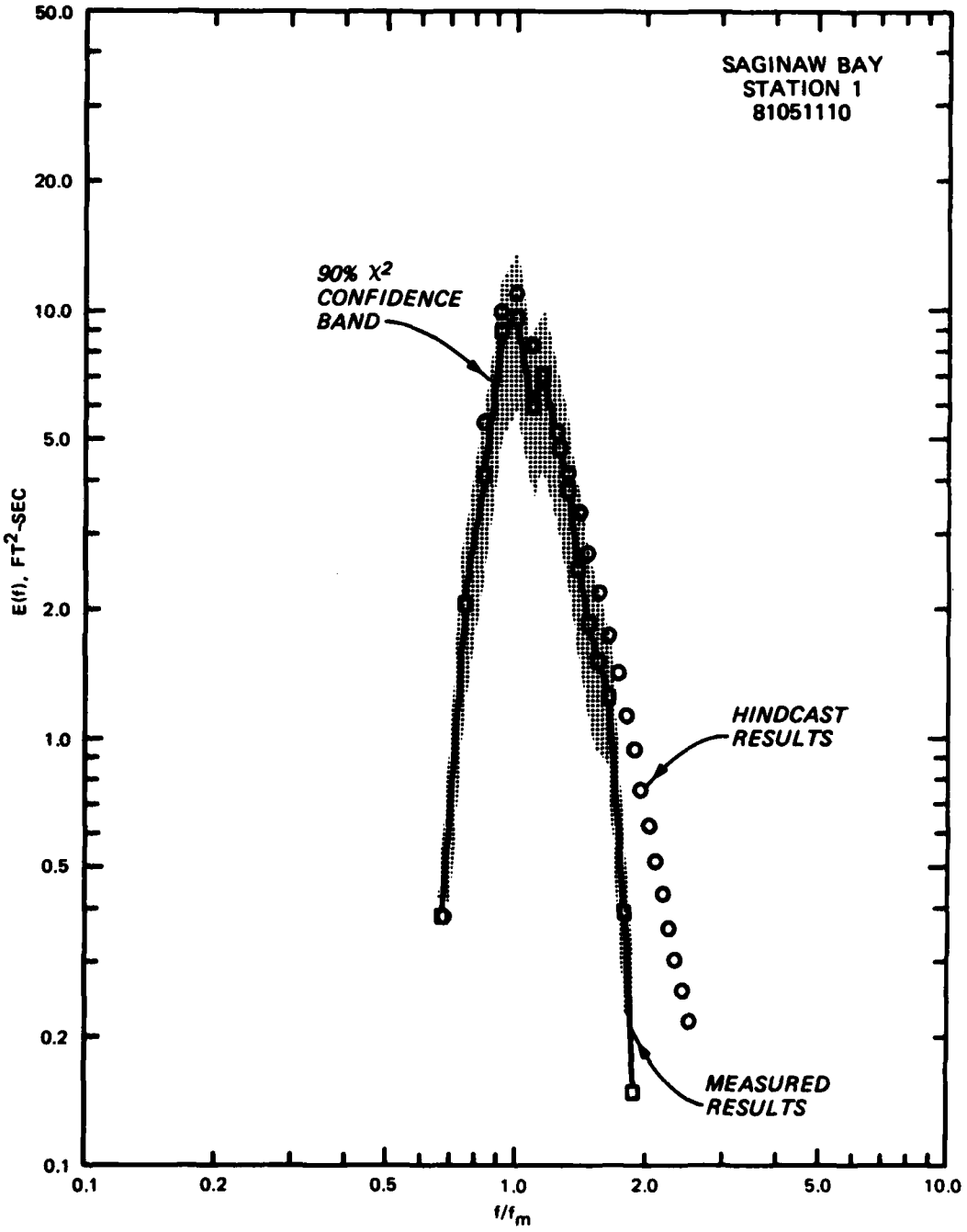


Figure 22. Comparison between measured and hindcast wave spectra, Station 1, 1000 hours, 11 May 1981

peak. The greatest discrepancy in the comparison of measured and hindcast peak frequencies was one discrete frequency band or 0.0156 Hz. Figures 18-22 show that from initial growth to final decay, the SWWM energy density spectrum follows the measured spectrum to within the 90 percent confidence limits. The forward face of the measured spectra conforms with the assumption of the spectral shape defined in Equation 19. The tail of the hindcast spectra conforms with the measured data except for small-scale temporal variations in the measured data and the extreme tail of the distribution, i.e., when $f/f_m > 2$. The discrepancy between the measured and hindcast spectra when $f/f_m > 2$ is a characteristic of a pressure sensing gage system such as used in this study. Assuming a linear transformation exists between the recorded pressure response and the free surface, individual wave component frequencies greater than 0.35 Hz will be increasingly damped with water depth. Thus representation of the energy density at frequencies greater than ≅0.35 Hz are very approximate. The relative energy at frequencies greater than 0.35 Hz is plotted but represents only an unknown fraction of the energy in a particular wave record.

31. The secondary peaks displayed in the measured spectra may be caused by several different mechanisms such as secondary wave trains propagating into the area or backscattering due to variations in bottom topography, the decomposition of finite amplitude waves into secondary harmonics, or an artifact of the analysis procedure.

32. Additional comparisons are also performed on three storms. For these comparisons, a secondary wind information data source was needed to supplement the Corps Saginaw Projects Office wind data. Wurtsmith Air Force Base, located near Oscoda, Michigan (44.4 deg N, 83.3 deg W), was able to provide wind data for the additional comparisons. These data, along with the data obtained at the Corps anemometer, suggest that the wind conditions over Saginaw Bay are nearly uniform. Moreover, the Wurtsmith wind records extend back over 20 years, thus providing a long-term data base suitable for hindcasting extremes.

33. The first comparison is made on storm conditions during 4-7 May 1981. The average wind speed during this period was approximately 15 mph, with maximum winds of 25 mph (Figure 23). The wind direction is shown to vary from due south to the northeast. Comparisons between the Corps and the Oscoda anemometers demonstrate that the wind data acquired at Wurtsmith Air Force Base can be used to provide an accurate representation of the wind

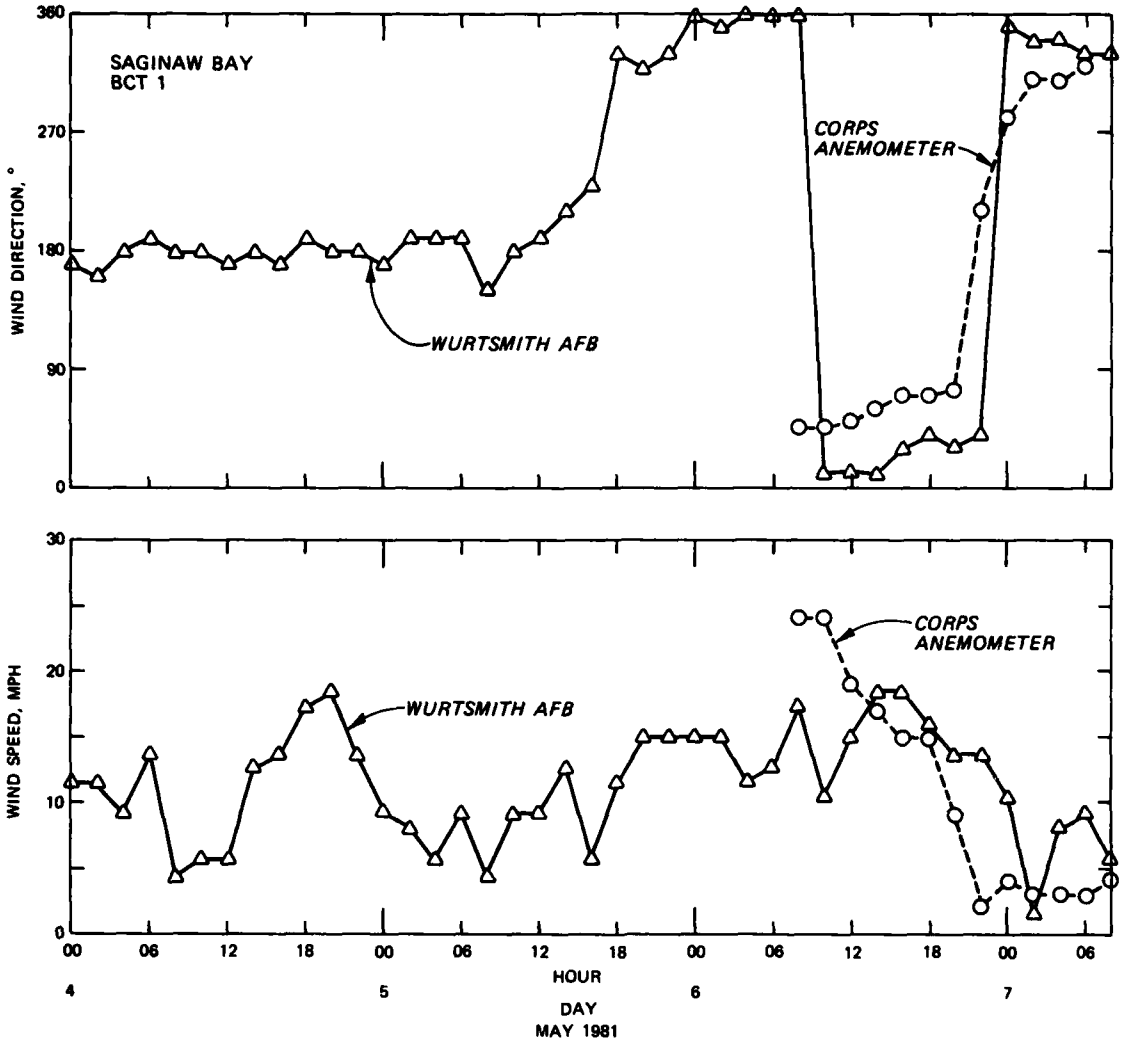


Figure 23. Comparison of wind records obtained at Wurtsmith AFB, Oscoda, Michigan, and CE Saginaw Projects Office, Essexville, Michigan

climate over Saginaw Bay. Figure 22 shows that the wind data acquired at these locations are virtually the same after adjustment for differences in their geographical locations. Figures 24 and 25 illustrate the results of the hindcast and measured wave conditions.

34. A second set of comparisons is made for a period of moderate winds which occurred during 8-10 October 1980. The wind data are presented in Figure 26, and again, there is good agreement between the data sets. The wind speed during this period averages about 8 mph with a maximum of about 15 mph. Results of the hindcast simulation using wind data from the Corps anemometer are presented in Figure 27. The relatively large discrepancies are probably

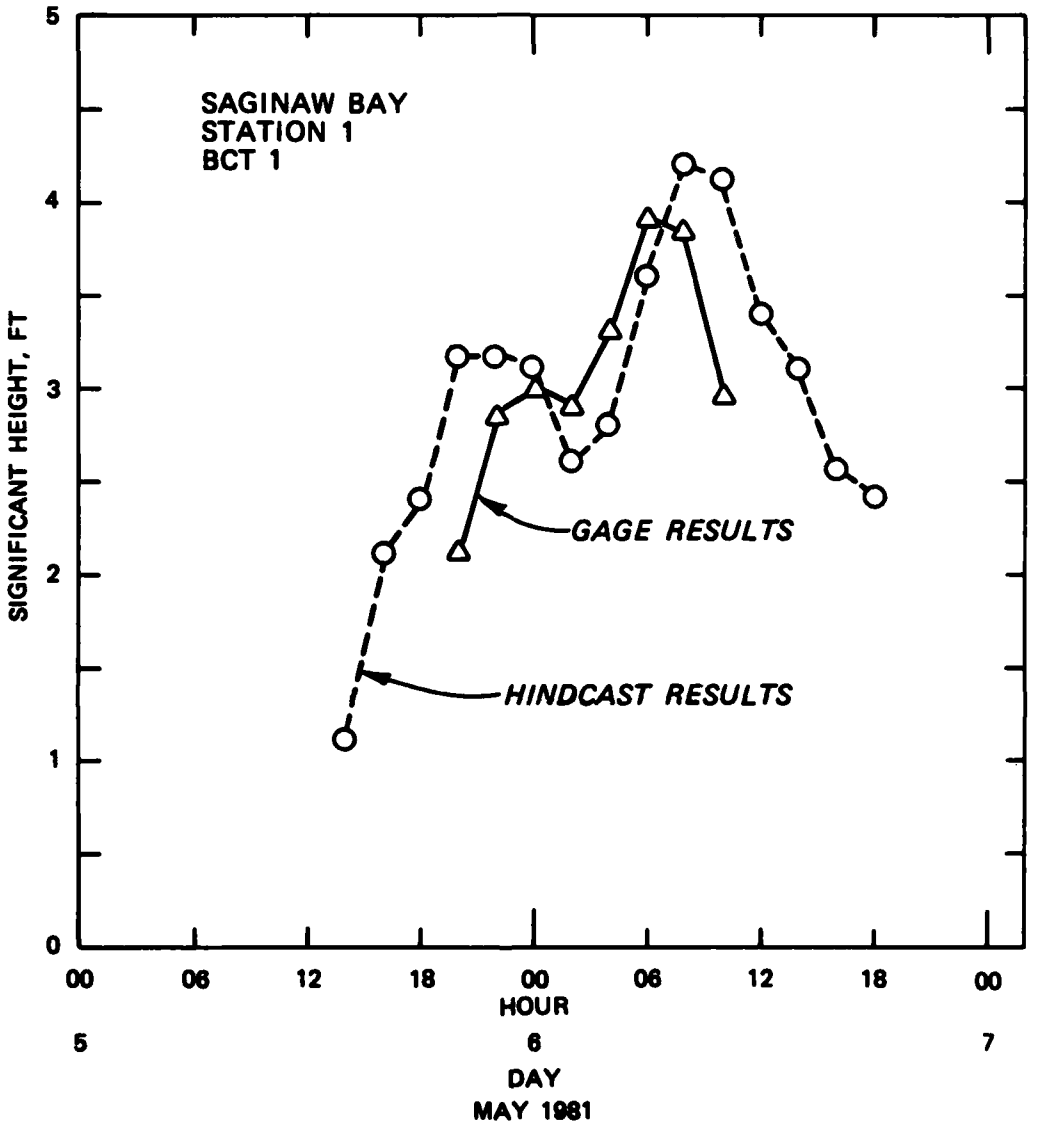


Figure 24. Comparison of measured and hindcast significant wave-height data, Station 1, 5-7 May 1981

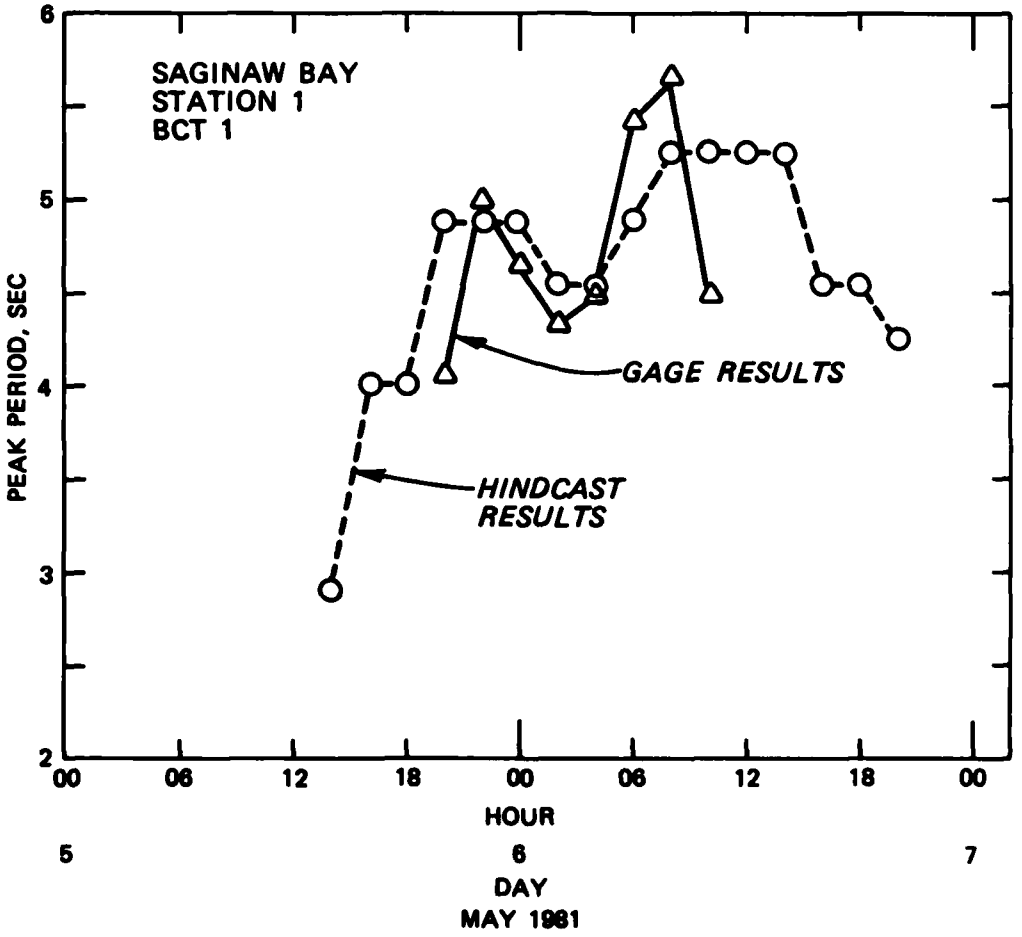


Figure 25. Comparison of measured and hindcast peak wave period, Station 1, 5-7 May 1981

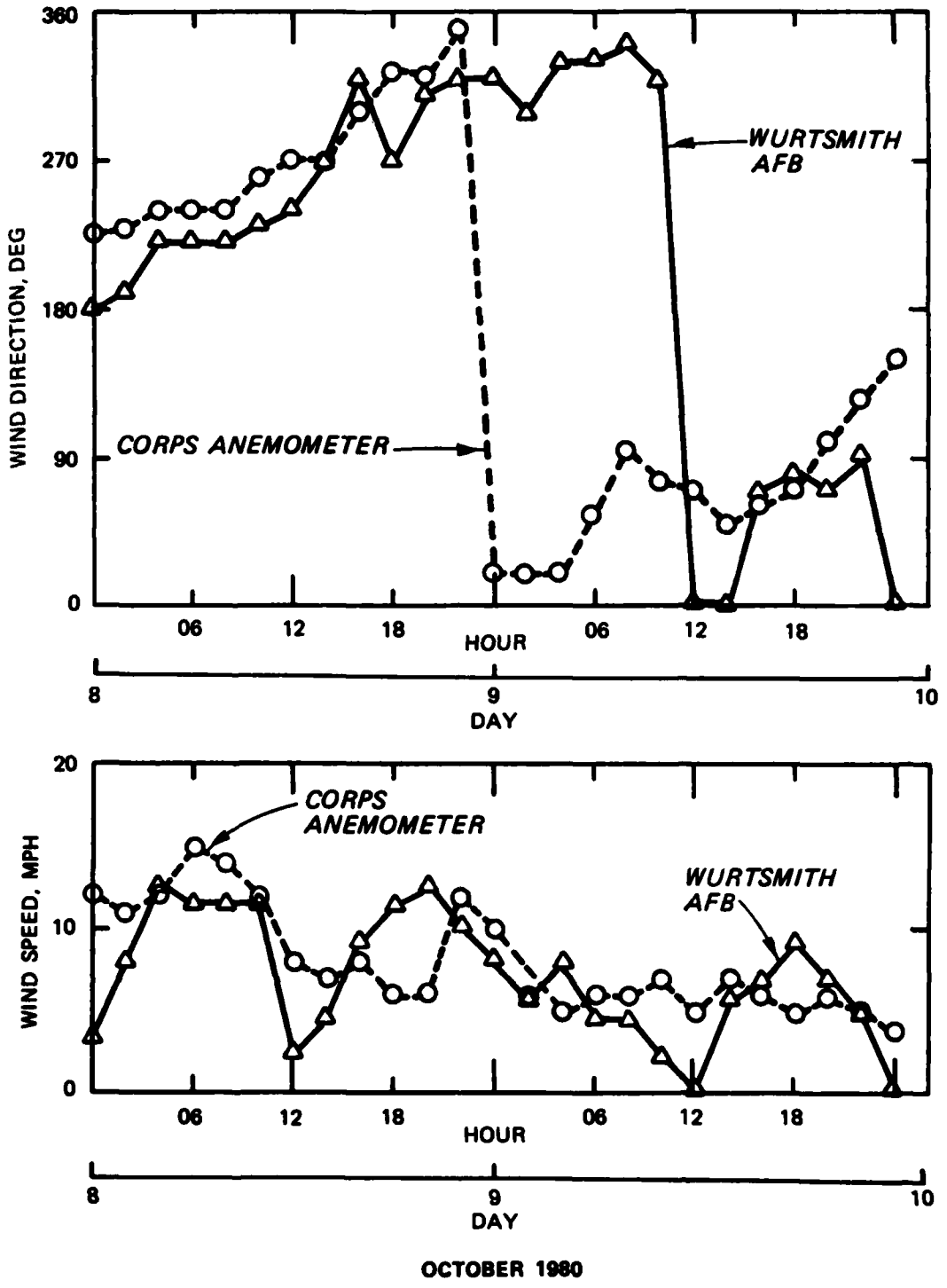


Figure 26. Comparison of wind data obtained at Wurtsmith AFB, Oscoda, Michigan, and CE Saginaw Projects Office, Essexville, Michigan, 8-10 October 1980

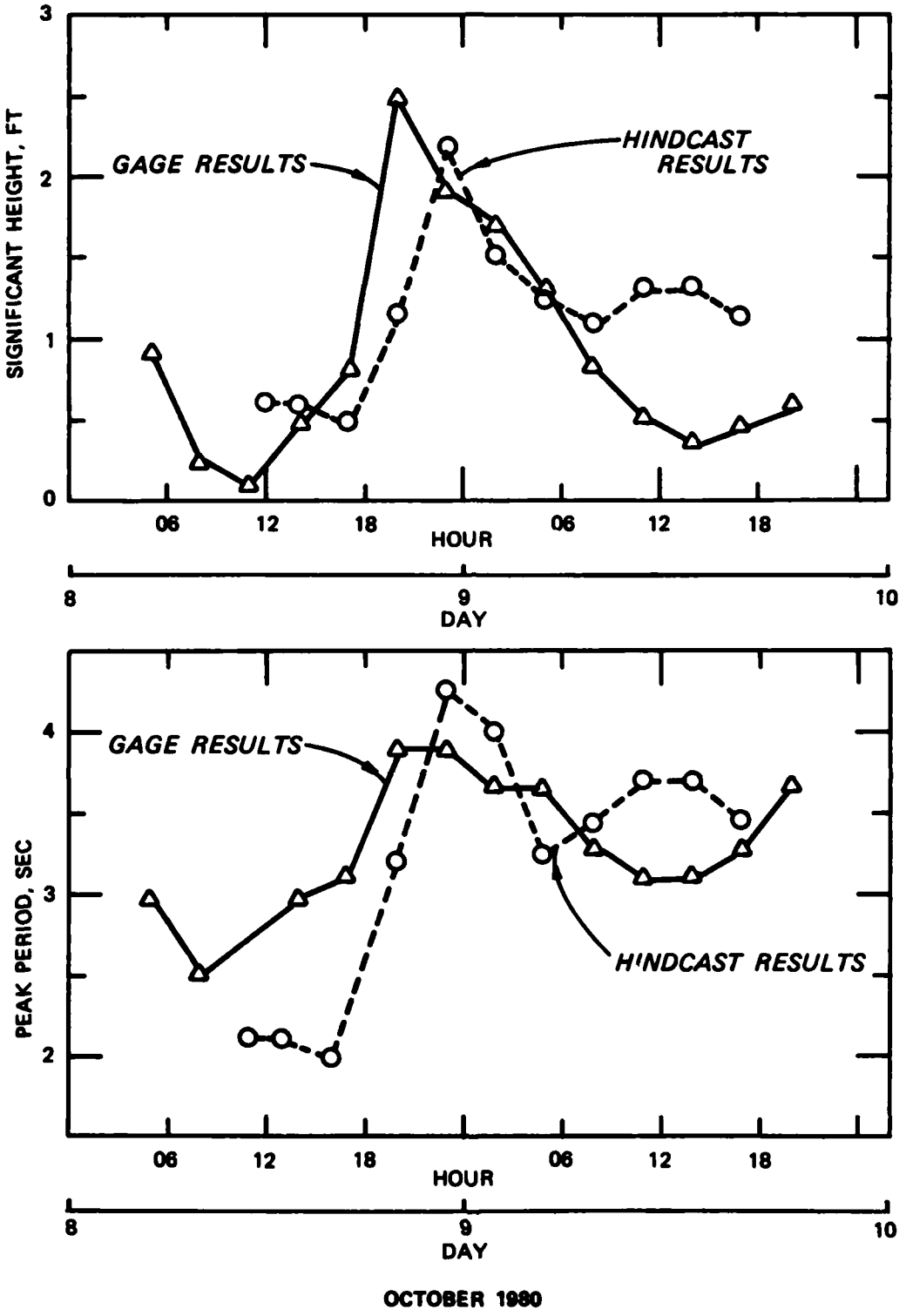


Figure 27. Comparison of measured and hindcast significant wave height and peak wave period for Station 1, 8-10 October 1980

the result of great variability in the wind direction during periods of low wind speeds.

35. Results of a third comparison using wind data shown in Figure 28 are shown in Figure 29. The wind data should be shifted approximately 14 hr to generate a wave climate to coincide with that observed. The necessity for shifting the wind data is probably caused by an incorrectly annotated wind record. Once adjusted in time (not shown in Figures 28 and 29), the discrepancies between the measured and hindcast data are within $\pm$0.5 ft for the significant height and $\pm$0.5 sec for the peak period.

36. Many more comparisons were performed than are presented here without adjustment of coefficients or modification to the hindcast model to account for changes in location. The comparisons convincingly demonstrate the ability of the SWWM to accurately hindcast wave conditions in Saginaw Bay to within $\pm$0.5 ft significant height and $\pm$1.0 sec peak period. Moreover, the theoretically derived spectral shapes generally conform within the 90 percent CHI-squared confidence limits of the measured spectra.

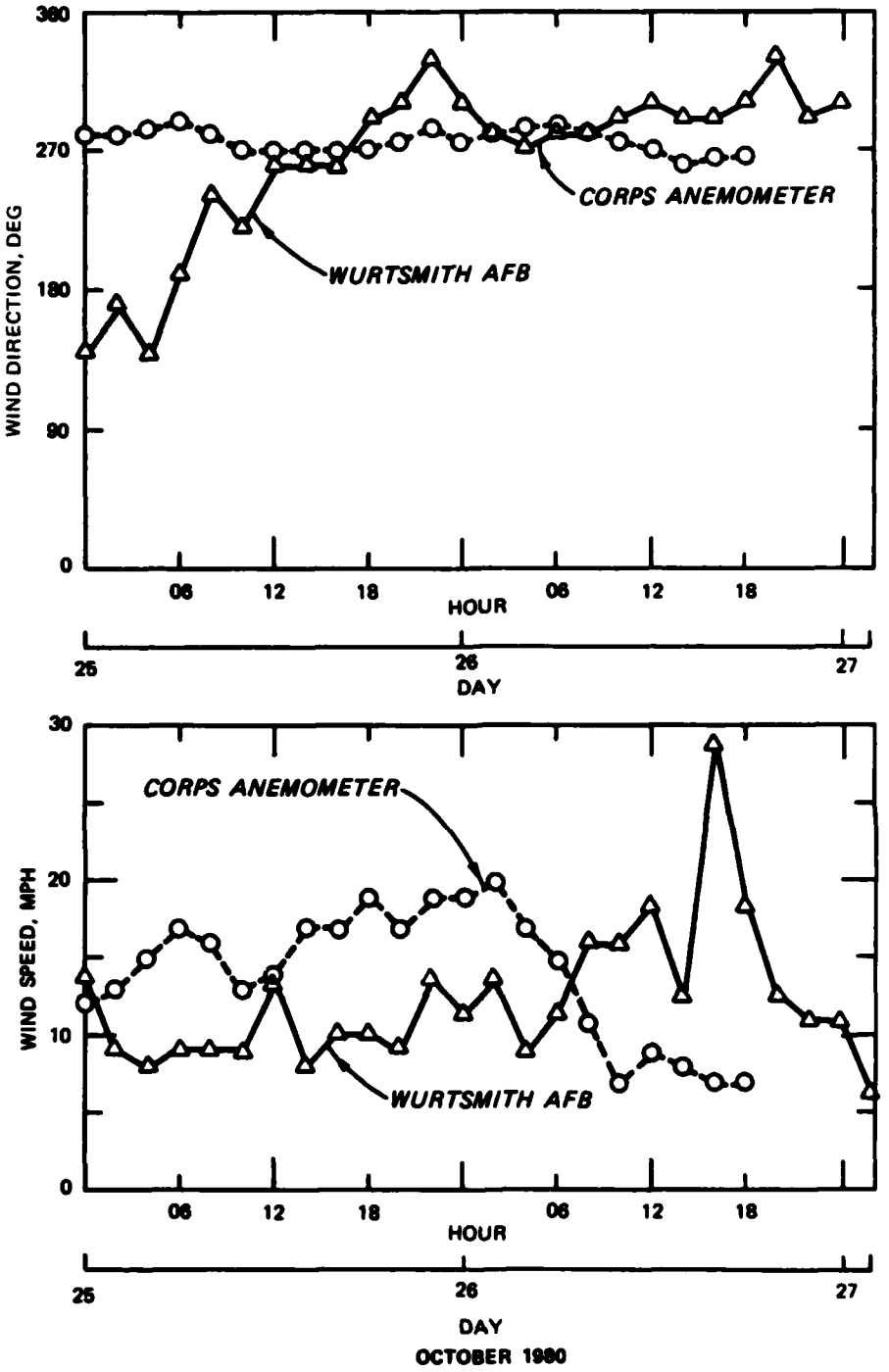


Figure 28. Comparison of wind data obtained at Wurtsmith AFB, Oscoda, Michigan, and CE Saginaw Projects Office, Essexville, Michigan, 25-27 October 1980

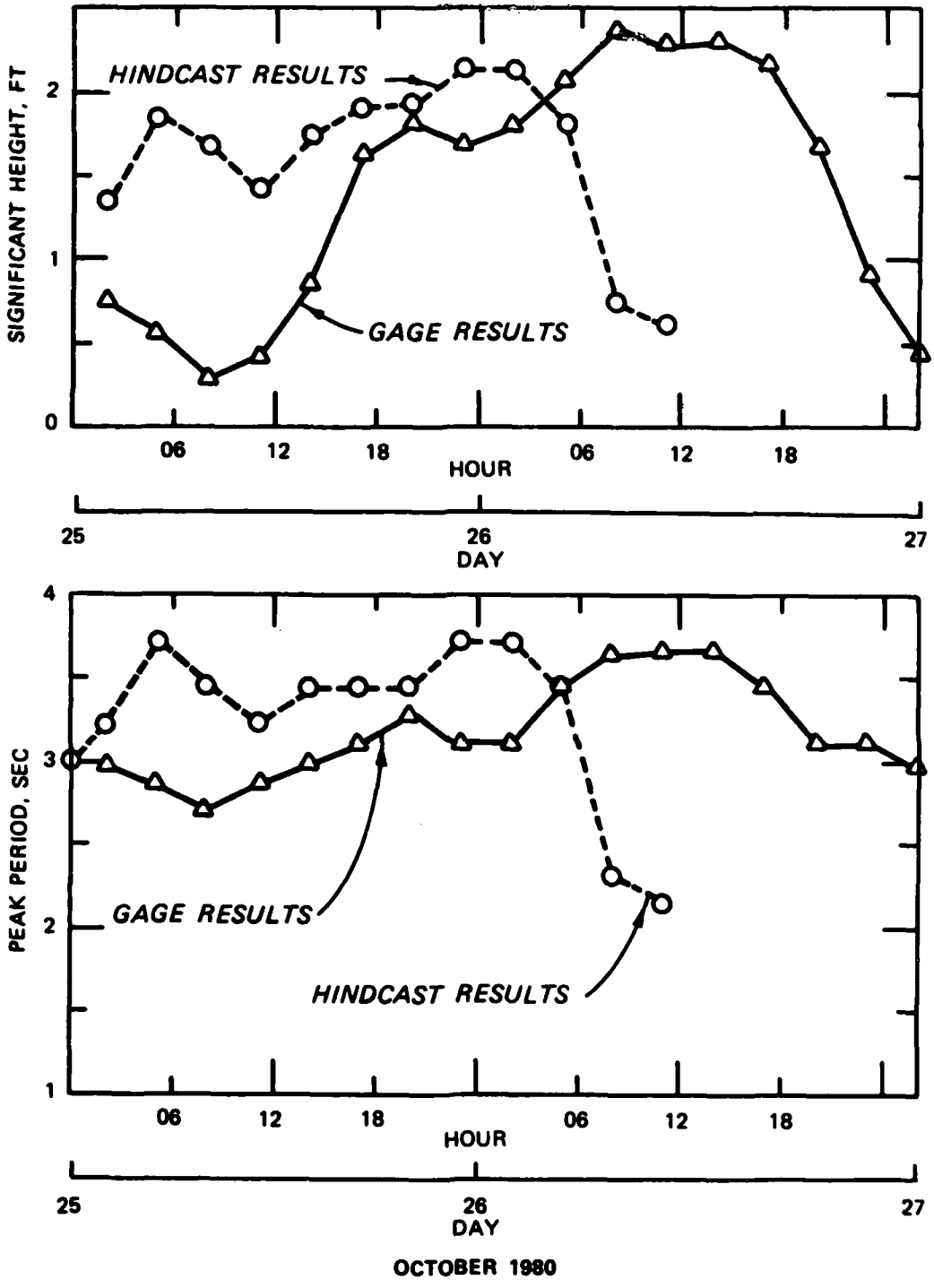


Figure 29. Comparison of measured and hindcast significant wave height and peak period for Station 1, 25-27 October 1980

## PART VI: GENERATION OF DESIGN WAVE CONDITIONS

37. Specification of a representative wind climate is necessary for the generation of design wave conditions in Saginaw Bay. The largest wind waves in the bay are generated by synoptic-scale systems such as extratropical cyclones. Smaller scale wind systems such as thunderstorms and squall lines are not large enough and do not persist long enough to generate a saturated wave field. Because of the mesoscale nature of the wind fields of interest, one or two wind records on the periphery of the bay are considered adequate to describe the wind field over the entire bay.

38. A recording anemometer system was installed in 1980 at the CE Saginaw Projects Office located near the mouth of the Saginaw Bay. Informal comparisons of the winds measured at the Saginaw Projects Office with those measured on the bay by ships operating in the area showed good agreement after the overwater to overland transformation was made. Records obtained at the Saginaw Projects Office were also compared with wind records obtained at Wurtsmith Air Force Base located near Oscoda, Michigan. The Wurtsmith records are particularly useful because there are over 20 years of data and thus provide a basis for the extremal analysis. Figure 23 shows a portion of a Wurtsmith wind record during a period in which data from the CE anemometer at Essexville, Michigan, were also available. The direction traces show good agreement considering the distance separating the stations. The speed traces agree less well but part of the disagreement can be accounted for in that the CE anemometer at Essexville is placed at a considerably higher elevation than the Wurtsmith anemometer.

39. Thus while the CE anemometer at Essexville provided the wind data for verification of the SWWM, the wind records obtained at Wurtsmith provide the basis for the extremal analysis.

40. In PART V, the SWWM was verified and a capability to hindcast the time-history of wave activity during individual storms was demonstrated. This capability permits the computation of extremal statistics if sufficient wind data are available. One of the major tasks of this study was locating sufficient wind data to confidently perform the analysis.

41. In PART V it was demonstrated that wind data obtained at Wurtsmith could be used to reliably hindcast wave conditions in Saginaw Bay. Twenty years of wind data (1950-1970) were requested and obtained from Wurtsmith.

The extremal hindcasts were performed under the following assumptions:

a. Wind speed and direction are held constant for each event.

b. The waves are generated under fetch-limited conditions.

The first step in the extremal analysis was to determine the wave heights produced by constant wind speed conditions for each azimuthal angle band. The angle bands selected cover 10 deg of azimuth. Figure 30 shows the results of this analysis; the highest $H_{m_0}$ values are generated by winds from the 20- to 40-deg azimuthal angle bands. The absolute maximum wave condition (Vincent 1981, Equation 21) of 7.9-ft significant wave height is generated when the wind speed attains 50 mph in these direction bands. There is a significant drop in the wave height in the 320-deg angle band caused by the limited fetch length and water depths that exist for that angle class. The data presented in Figure 30 should not be used for design purposes. The $H_{m_0}$ results are generated for very specific wind conditions that may not have occurred in nature. The curves are used in this case to further quantify extreme storm conditions for given wind speeds and principal wind directions. Once the maximum wave-producing angle bands are known, it becomes a matter of searching the 20-year wind record for wind conditions in the 20- to 40-deg angle bands and wind speeds greater than 25 knots.* Of a total of 153,298 observations, 631 recorded wind speeds greater than 25 knots for all direction bands (Table 1). Of the 631 observations, five wind conditions were selected that as a group, produced the most severe wave conditions. The "most severe" is not to say that no greater conditions existed; simply that the anemometer may not have been in continuous operation during such periods. The wind conditions producing the most severe wave conditions are shown in Table 2.

42. The time-histories of the storms are provided in Appendix A (Figures A1-A10). The wind speed and direction were averaged over 2-hr intervals. Wind data for the five storm conditions were used to drive the SWWM to compute $H_{m_0}$ and $T_p$. The winds were corrected for differences in anemometer heights and converted to overwater winds according to the procedure described by Resio and Vincent (1976) and U. S. Army CERC, CETN-I-5 (1981a). The winds and corresponding wave conditions are displayed in Figures A1-A10. Table 3 is a tabulation of the maximum significant wave-height conditions computed using the SWWM.

---

* Wurtsmith Air Force Base recorded the wind data in units of whole knots.

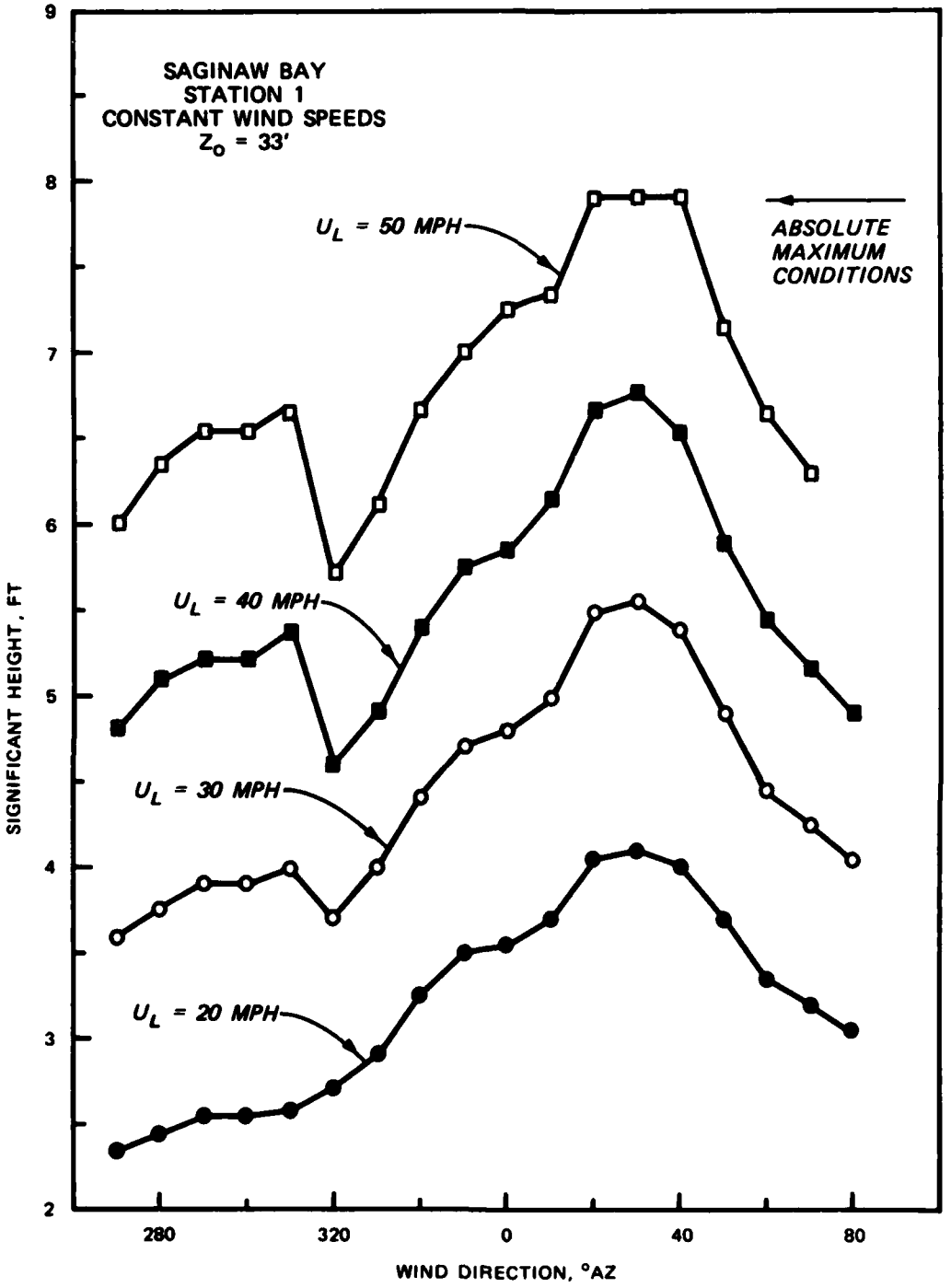


Figure 30. Hindcast wave heights as a function of wind speed and direction

Table 1

Percent Occurrence of Wind Conditions for Wurtsmith Air Force Base 1950-1970

(Percent Occurrence Times 1000)

| Wind Speed knots | Wind Direction, degrees azimuth | | | | | | | | |
|---|---|---|---|---|---|---|---|---|---|
| | 0-22 | 22-45 | 45-67 | 67-90 | 90-112 | 112-135 | 135-157 | 157-180 | 180-202 |
| 25-29.9 | 40 | 57 | 35 | 14 | 8 | 1 | 2 | 1 | 5 |
| 30-34.9 | 8 | 12 | 10 | 2 | 1 | 1 | -- | -- | -- |
| 35-39.9 | 1 | 3 | 6 | 1 | -- | -- | -- | -- | -- |
| 40-44.9 | -- | -- | -- | -- | -- | -- | -- | -- | -- |
| 45-49.9 | -- | -- | -- | -- | -- | -- | -- | -- | -- |
| 50-Greater | -- | -- | 1 | -- | -- | -- | -- | -- | -- |
| Total | 49 | 72 | 52 | 17 | 9 | 2 | 2 | 1 | 5 |

| Wind Speed knots | Wind Direction, degrees azimuth | | | | | | | |
|---|---|---|---|---|---|---|---|---|
| | 202-225 | 225-247 | 247-270 | 270-292 | 292-315 | 315-337 | 337-360 | Total |
| 25-29.9 | 13 | 37 | 20 | 11 | 12 | 44 | 37 | 337 |
| 30-34.9 | 1 | 8 | 1 | 1 | 2 | 5 | 5 | 57 |
| 35-39.9 | -- | 4 | 1 | -- | -- | -- | -- | 16 |
| 40-44.9 | -- | -- | -- | -- | -- | -- | -- | -- |
| 45-49.9 | -- | -- | -- | -- | -- | -- | -- | -- |
| 50-Greater | -- | -- | -- | -- | -- | -- | -- | 1 |
| Total | 14 | 49 | 22 | 12 | 14 | 49 | 42 | 411 |

Note: Total number of observations greater or equal to 25 knots = 631.
Total number of observations from 1950-1970 = 153,298.

Table 2

Storm Conditions for Extreme Analysis

| Storm Number | Date of Storm | | |
|---|---|---|---|
| 1 | 51-10-31-01 | to | 51-11-01-00 |
| 2 | 58-11-18-00 | to | 58-11-20-00 |
| 3 | 58-11-26-00 | to | 58-11-30-00 |
| 4 | 64-04-13-00 | to | 64-04-16-00 |
| 5 | 68-04-04-00 | to | 68-04-12-00 |

Table 3

Maximum Significant Wave Heights Computed Using External Wind Data

| Storm Number | $H'_{m_0}$, ft | $\bar{H}^{*}_{m_0}$, ft, and $\sigma^2$ |
|---|---|---|
| 1 | 7.1 | 5.5 ± 1.3 |
| 2 | 6.3 | 5.1 ± 1.3 |
| 3 | 6.7 | 5.8 ± 0.7 |
| 4 | 6.4 | 5.4 ± 1.2 |
| 5 | 6.9 | 5.6 ± 1.0 |

* $\bar{H}_{m_0}$ is the mean significant wave height determined from wave conditions ± 4 hr from $H'_{m_0}$; $\sigma^2$ is the variance about the mean $H_{m_0}$ (or $\bar{H}_{m_0}$).

43. Although arguments can be made for ranking the storms by either $H'_{m_0}$ or $\bar{H}_{m_0}$, the latter ranking is used in this study because of the exaggerated influence of possible wind errors. Consider the maximum $H_{m_0}$, 7.1 ft, found in the first storm which was generated using a windspeed of 37 knots. The 37-knot wind speed was calculated by averaging wind speeds $\pm$1.0 hr around a given time t as

$$\bar{U}_t = \frac{1}{3}\left(U_{t-1} + U_t + U_{t+1}\right) \tag{22}$$

The three values employed for $U_{t-1}$, $U_t$, and $U_{t+1}$ were 25, 50, and 36 knots, respectively. It appears that the 50-knot wind speed, of which there is only one value in the 20-year record, may be incorrect or a short gust unrepresentative of the synoptic scale winds. Thus Table 4 shows the storms ranked according to the $\bar{H}_{m_0}$ value with return period

$$T_R = \frac{1/R}{1 + NY} \tag{23}$$

where

$T_R$ = the return period

R = the storm rank

NY = the duration of the data base in years

These data, along with the $H'_{m_0}$ return period, are displayed in Figure 31.

Table 4

Storm Ranking and Return Period

| Rank | $\bar{H}_{m_0}$, ft | Storm Number | Return Period, year |
|---|---|---|---|
| 1 | 5.8 | 3 | 21 |
| 2 | 5.6 | 5 | 10.5 |
| 3 | 5.5 | 1 | 7 |
| 4 | 5.4 | 4 | 5.3 |
| 5 | 5.1 | 2 | 4.2 |

44. Two additional storm-related $H_{m_0}$ values are presented in Figure 31: the maximum wave condition occurring during the 10 May 1981 storm

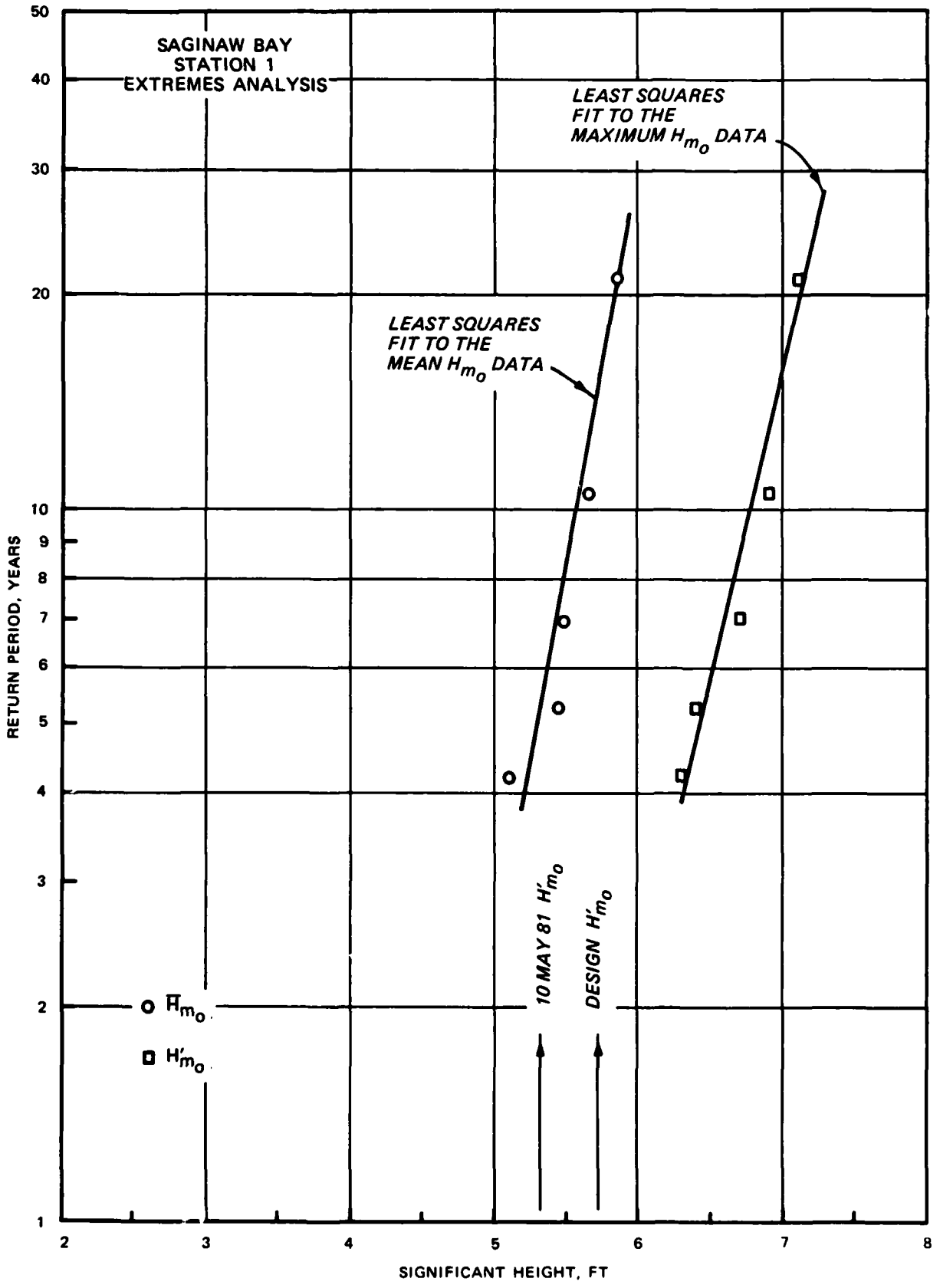


Figure 31. Return periods for mean and maximum significant wave height

(measured), and the design maximum wave condition (NCE*) used for the construction of the retaining structure. It is evident that both $H'_{m_0}$ conditions are considerably smaller than the $H_{m_0}$ conditions hindcast for maximum storm related $H_{m_0}$ data. Comparison of the two data points versus the mean $H_{m_0}$ data shows that the resulting return period would be approximately 6 years (10 May 1981 storm) and 15 years (design wave condition). Although the 10 May 1981 storm generated the largest $H_{m_0}$ conditions recorded, they are, in comparison with historical data, of relatively small magnitude.

45. Additional estimates of extreme wave conditions can be obtained employing an assumed statistical distribution of the waves within a given recording period. A Rayleigh distribution has normally been assumed to represent the observed wave conditions (U. S. Army CERC 1977). From this assumption, a relationship is obtained relating $H_{m_0}$ to $H_{1/100}$ (where $H_{1/100}$ is the average of the highest 1 percent of all waves), or

$$H_{1/100} = \varepsilon H_{m_0}$$

where $\varepsilon$ is equal to 1.67. Care must be employed when using the above equation since the $H_{m_0}$ results are theoretically limited (and physically limited) by the waterdepth (Equation 21) and also saturation conditions (Figure 31). Therefore $H_{1/100}$ will be limited in a similar manner as $H_{m_0}$ When $H_{m_0}$ approaches its theoretical maximum condition (approximately 7.9 ft) the assumed Rayleigh distribution will no longer hold; the tail of the distribution would be truncated at some wave height (Baitjes 1972 and Goda 1975). When this occurs $\varepsilon$ will diverge from the assumed wave of 1.67 and approach 1.0.

---

* P. McCallister. 1979. Letter, "Subject: Saginaw Diked Disposal Facility," U. S. Army NCE, Detroit, Mich.

## PART VII: SUMMARY AND CONCLUSIONS

46. A wave-measurement system was deployed in Saginaw Bay, Michigan, in the fall of 1979 and operated during the ice-free parts of the spring and fall seasons of 1980 and 1981. Concurrently, development of a numerical wave hindcast model capable of simulating wind-wave generation in shallow water was completed.

47. The most severe and definitive storm during the measurement period occurred in May 1981. While the wind speeds recorded during this storm were not particularly high (30 to 35 mph), they were very uniform in terms of both speed and direction. Moreover, the predominant direction was parallel to the major axis of the bay thereby allowing the greatest fetch length. The conditions that occurred during this storm resulted in a near ideal wave data set for verifying the Shallow-Water Wave Model (SWWM). All three gages performed almost perfectly and data recovery was nearly 100 percent. The near stationary wind field permitted a definitive test of correct simulation of growth with fetch and growth with time of the SWWM. Results of the verification are presented herein and demonstrate the ability of the SWWM to reproduce both the total energy and peak frequency of the measured spectra.

48. Review of 20 years of wind data obtained at Wurtsmith Air Force Base near Oscoda, Michigan, disclosed five storms that occurred between 1950 and 1970 suitable to use as a basis for an extremal analysis. In the 20 years of recorded data, there was one occurrence of a 50-mph wind speed. Hindcast simulation using this wind speed showed the wave field to reach a saturated condition at about 7.9-ft maximum wave height. Thus it appears the maximum wave height to be expected at the disposal facility is about 8 ft.

49. There have been informal reports of sustained wind speeds greater than 60 mph measured prior to the inception of the wave-measurement program. It is recommended that the wind measurement system installed at the Saginaw Projects Office continue in operation indefinitely. Wind data of this nature will provide very valuable information on the frequency of occurrence of very high wind speeds and may lead to revision of the table of return periods for large wave heights.

# REFERENCES


Baitjes, J. A. 1972. "Set-Up due to Irregular Waves," Report No. 72-2, Communications on Hydraulics, Delft University of Technology, Department of Civil Engineering, Delft, The Netherlands.

Bretschneider, C. L. 1952. "The Generation and Decay of Wind Waves in Deep Water," Transactions, American Geophysical Union, Vol 33, No. 3, pp 381-389.

Bretschneider, C. L., and Reid, R. O. 1954. "Changes in Wave Height due to Bottom Friction, Percolation and Refraction," Technical Memorandum No. 45, Beach Erosion Board.

Goda, Y. 1974. "Estimation of Wave Statistics from Spectral Information," Proceedings, International Symposium on Ocean Wave Measurement and Analysis, American Society of Civil Engineers, Vol 1, pp 320-337.

_____. 1975. "Irregular Wave Deformation in the Surf Zone," Coastal Engineering in Japan, Vol 18, pp 13-26.

Hasselmann, K. 1962. "On the Non-Linear Energy Transfer in a Gravity Wave Spectrum-General Theory," Journal of Fluid Mechanics, Vol 12, Part 1, pp 481-500.

Hasselmann, K., et al. 1973. "Measurements of Wind-Wave Growth and Swell Decay During the Joint North Sea Wave Project JONSWAP," Dtsch, Hydrogr. Z., Vol 8, Supplement A8, No. 12.

_____. 1976. "A Parametric Wave Prediction Model," Journal of Physical Oceangraphy, Vol 6, pp 200-228.

Iwata, Koichird. 1980. "Wave Spectrum Changes due to Shoaling and Breaking; I, Minus - Three - Power - Law on Frequency Spectrum," Osaka University, Technical Report, Vol 30, No. 1517-1550, pp 269-278.

Jensen, R. E. "Methodology for the Calculation of a Shallow-Water Wave Climate," WIS Report 8 (in preparation), U. S. Army Engineer Waterways Experiment Station, CE, Vicksburg, Miss.

Johnson, J. W., O'Brien, M. P., and Isaacs, J. D. 1948. "Graphical Construction of Wave Refraction Diagrams," HO No. 605, TR-2, U. S. Naval Oceanographic Office, Washington, D. C.

Kitaigordskii, S. A. 1962. "Application of the Theory of Similarity to the Analysis of Wind-Generated Wave Motion as a Stochastic Process," Bull. Acad. Sci. USSR Ser. Geophys., Vol 1, No. 1, pp 105-117.

Kitaigordskii, S. A. , Krasitskii, V. P., and Zaslavaskii, M. M. 1975. "On Philips' Theory of Equilibrium Range in the Spectra of Wind-Generated Gravity Waves," Journal of Physical Oceanography, Vol 5, pp 410-420.

Mitsuyasu, Hisashi. 1968. "On the Growth of the Spectrum of Wind-Generated Waves (I)," Reports of Research Institute for Applied Mechanics, Kysusha University, Vol 16, No. 55, pp 459-482.

_____. 1969. "On the Growth of the Spectrum of Wind-Generated Waves (II)," Reports of Research Institute for Applied Mechanics, Kysusha University, Vol 17, No. 59, pp 235-248.

Mitsuyasu, Hisashi, and Kirmura, Hisao. 1965. "Wind Wave in Decay Area," Coastal Engineering in Japan, Vol 8, pp 221-35.

Ou, Shan-Hwei. 1980 (Sep). "The Equilibrium Range in the Frequency Spectra of the Wind Generated Gravity Waves," Proceedings, Fourth Conference on Ocean Engineering in the Republic of China.

Phillips, O. M. 1957. "On the Generation of Waves by Turbulent Wind," Journal of Fluid Mechanics, Vol 2, pp 417-445.

_____. 1958. "The Equilibrium Range in the Spectrum of Wind-Generated Waves," Journal of Fluid Mechanics, Vol 4, pp 426-434.

Resio, D. T. and Vincent, C. L. 1976 (Jun). "Estimation of Winds over the Great Lakes," Miscellaneous Paper H-76-12, U. S. Army Engineer Waterways Experiment Station, CE, Vicksburg, Miss.

Thornton, E. B. 1977. "Rederivation of the Saturation Range in a Frequency Spectrum of Wind-Generated Gravity Waves," Journal of Physical Oceanography, Vol 7, pp 137-140.

U. S. Army Coastal Engineering Research Center, CE. 1977. Shore Protection Manual, 3rd ed. (Vols I, II, and III), Stock No. 008-022-00113-1, U. S. Government Printing Office, Washington, D. C.

_____. 1981a. "Method of Determining Adjusted Windspeed, UA, for Wave Forecasting," CETN-I-5, Fort Belvoir, Va.

_____. 1981b. "Revised Method for Wave Forecasting in Shallow Water," CETN-I-6, Fort Belvoir, Va.

Vincent, C. L. 1981. "A Method for Estimating Depth-Limited Wave Energy" (in preparation), U. S. Army Coastal Engineering Research Center, CE, Fort Belvoir, Va.

Vincent, C. L., and Lichy, D. E. 1981. "ARSLOE Wave Measurements," Proceedings, Conference on Directional Wave Spectra Applications, American Society of Civil Engineers, pp 71-86.

# APPENDIX A: WIND AND WAVE DATA OF STORM CONDITIONS USED IN EXTREMAL ANALYSIS

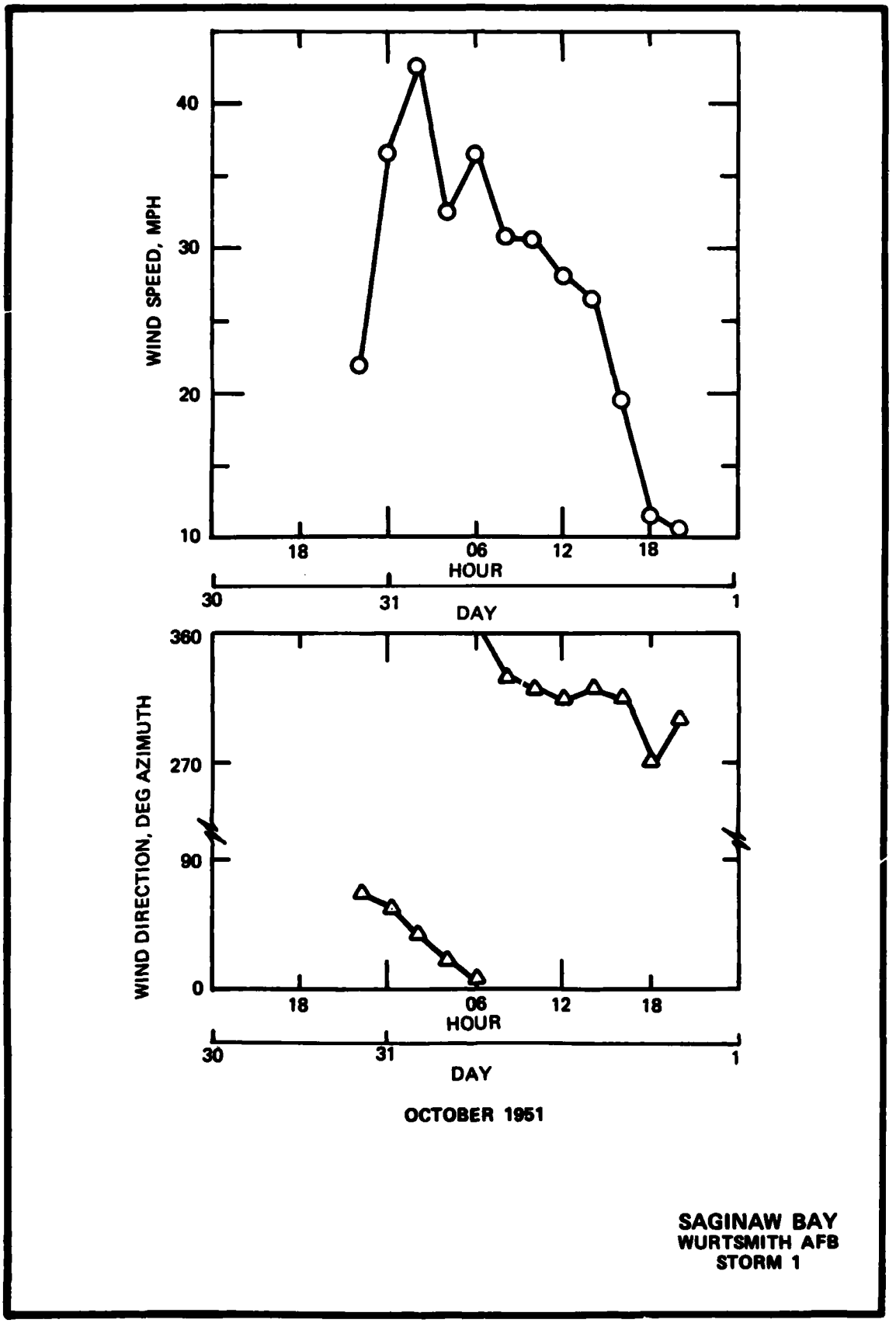


Figure A1. Wind data used for hindcast of storm of 30 October to 1 November 1951

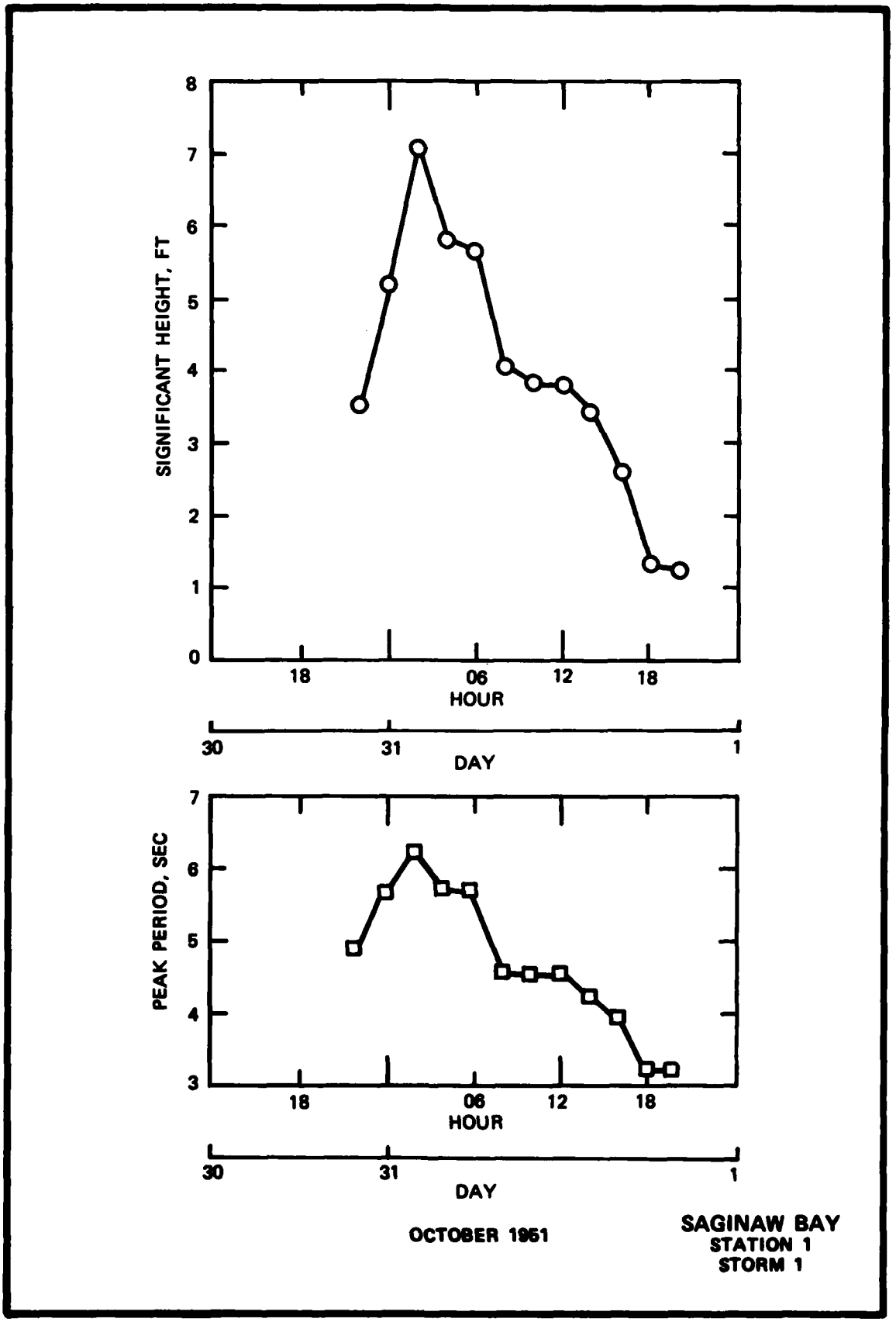


Figure A2. Hindcast significant wave height and peak wave period for storm of 30 October to 1 November 1951

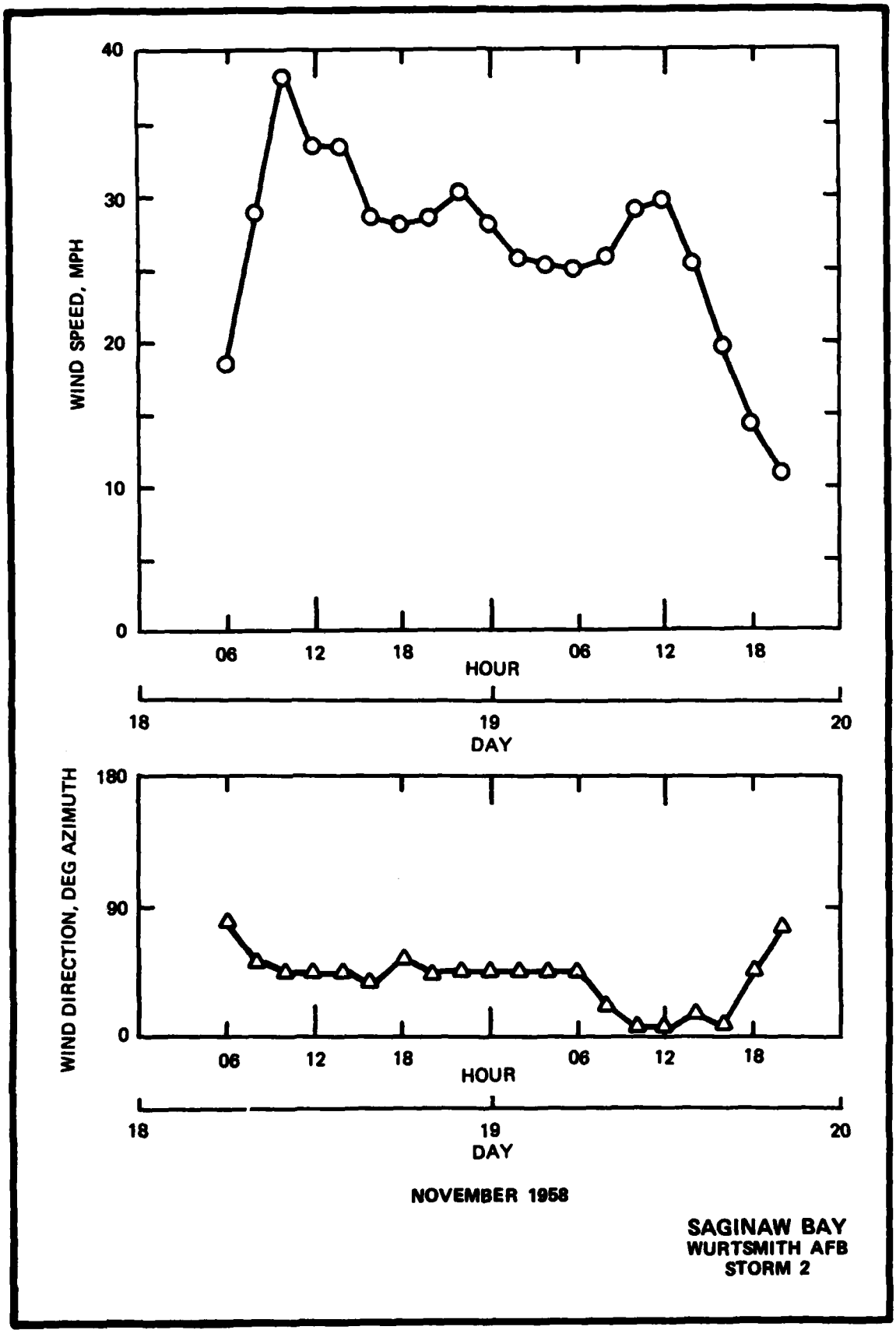


Figure A3. Wind data used for hindcast of storm of 18-20 November 1958

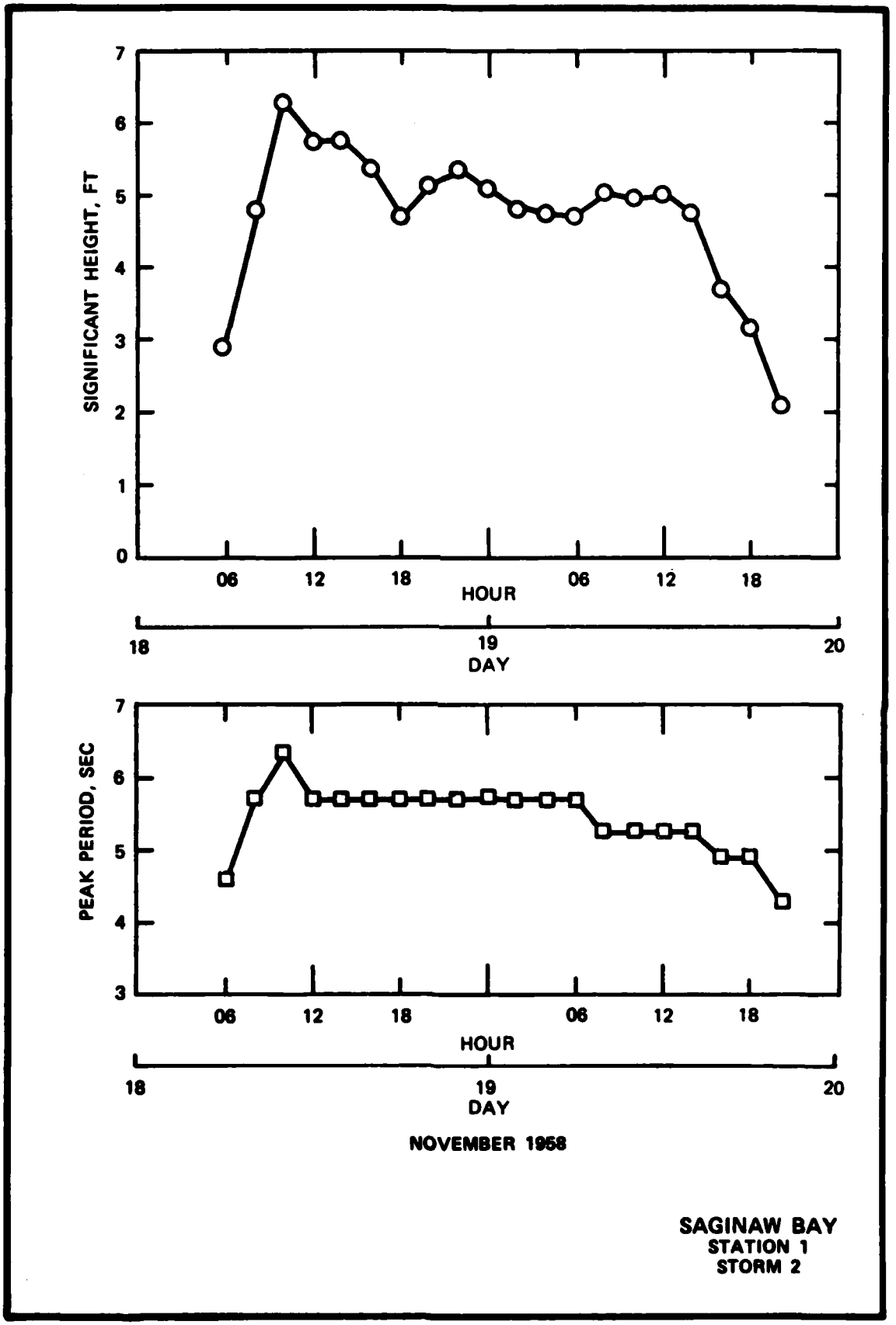


Figure A4. Hindcast significant wave height and peak wave period for storm of 18-20 November 1958

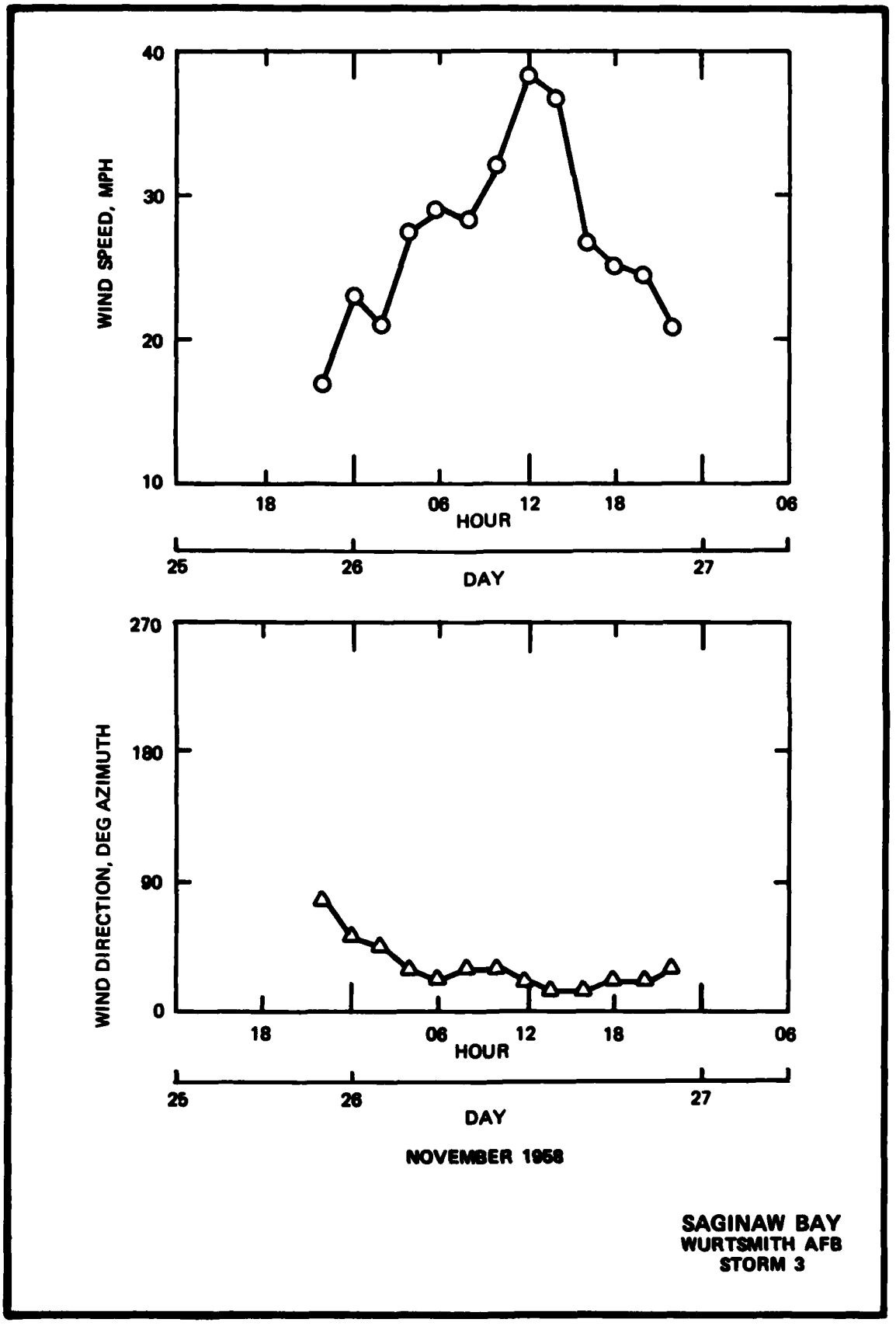


Figure A5. Wind data used for hindcast of storm of 25-27 November 1958

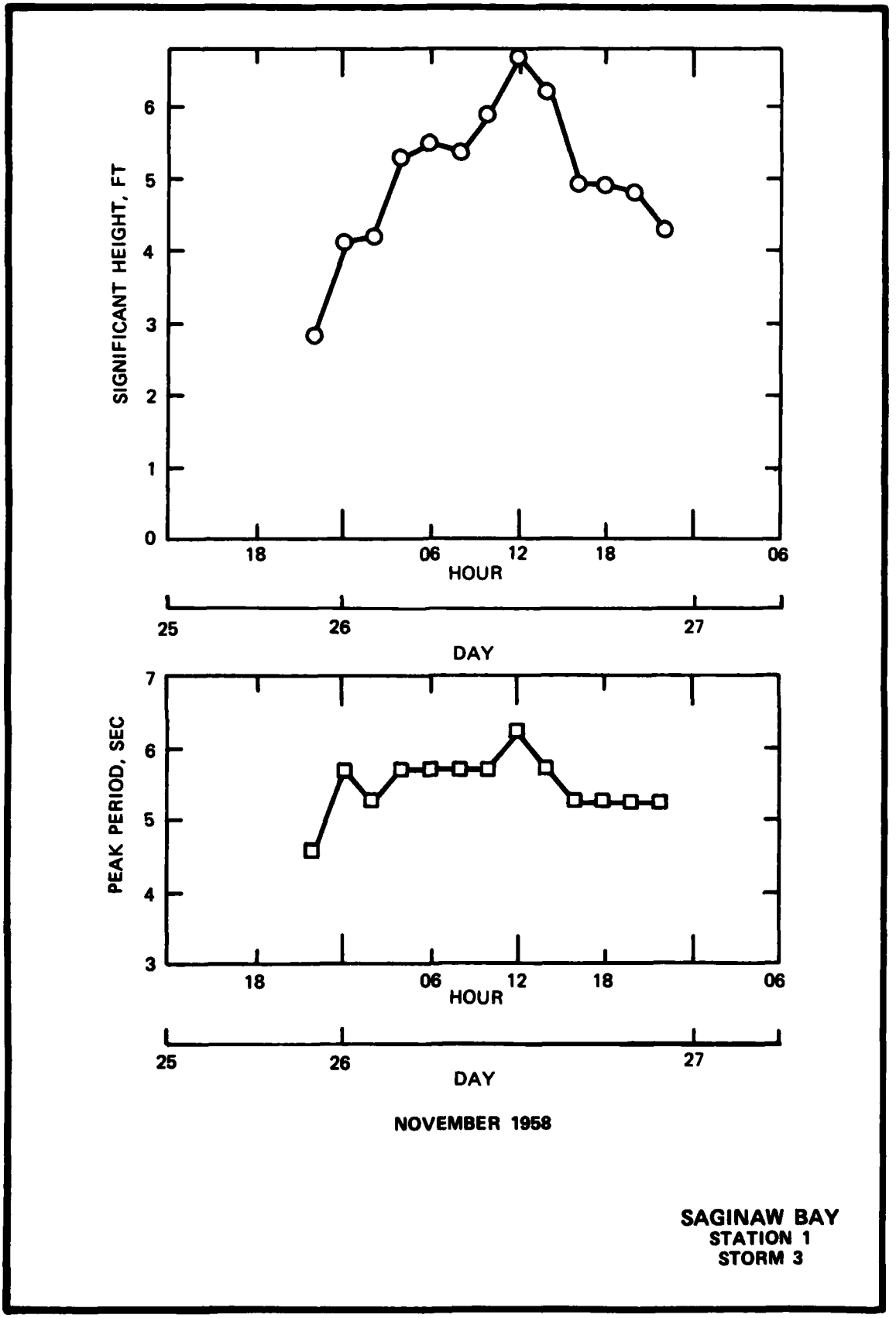


Figure A6. Hindcast significant wave height and peak wave period for storm of 25-27 November 1958

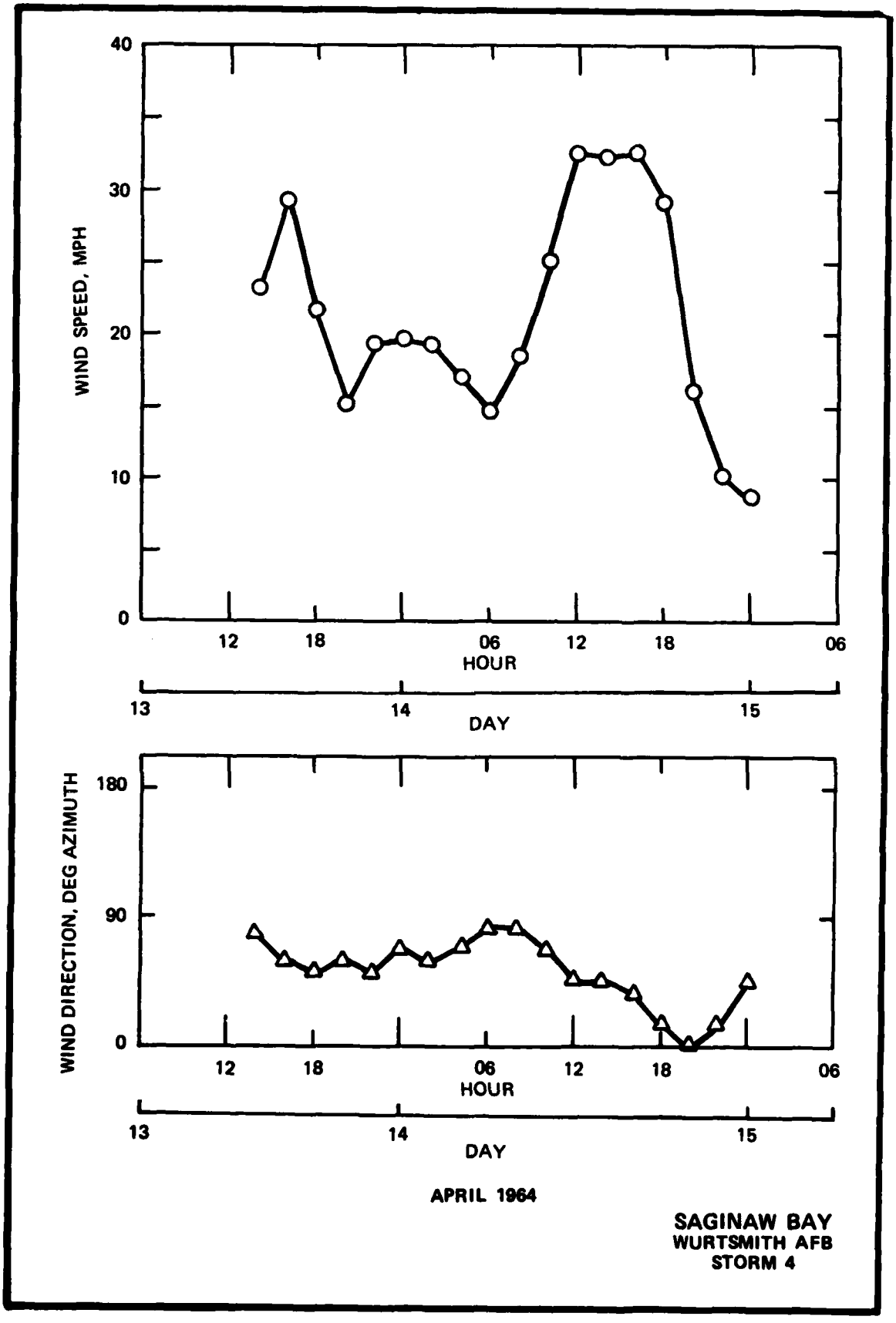


Figure A7. Wind data used for hindcast of 13-15 April 1964

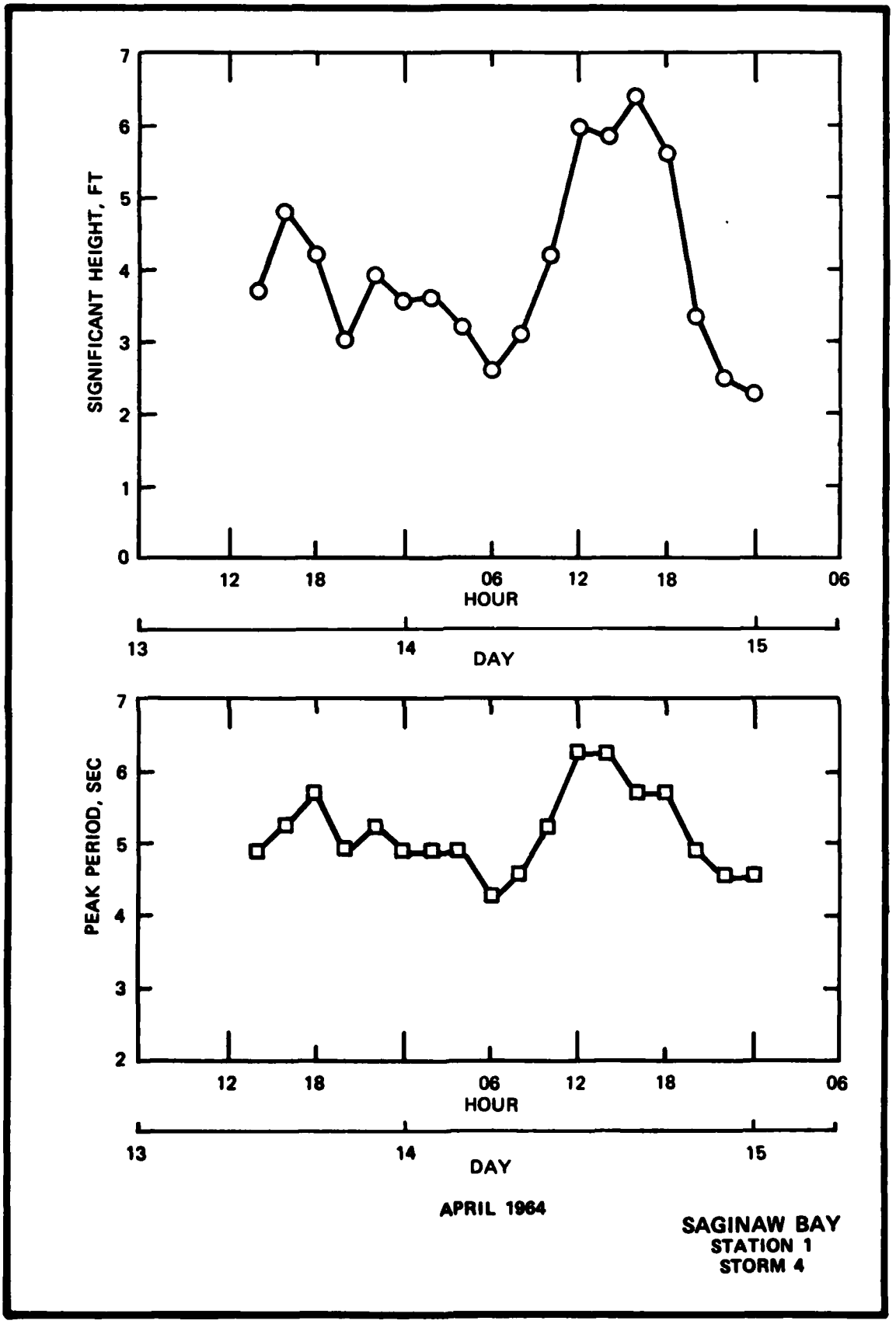


Figure A8. Hindcast significant wave height and peak wave period for storm of 13-15 April 1964

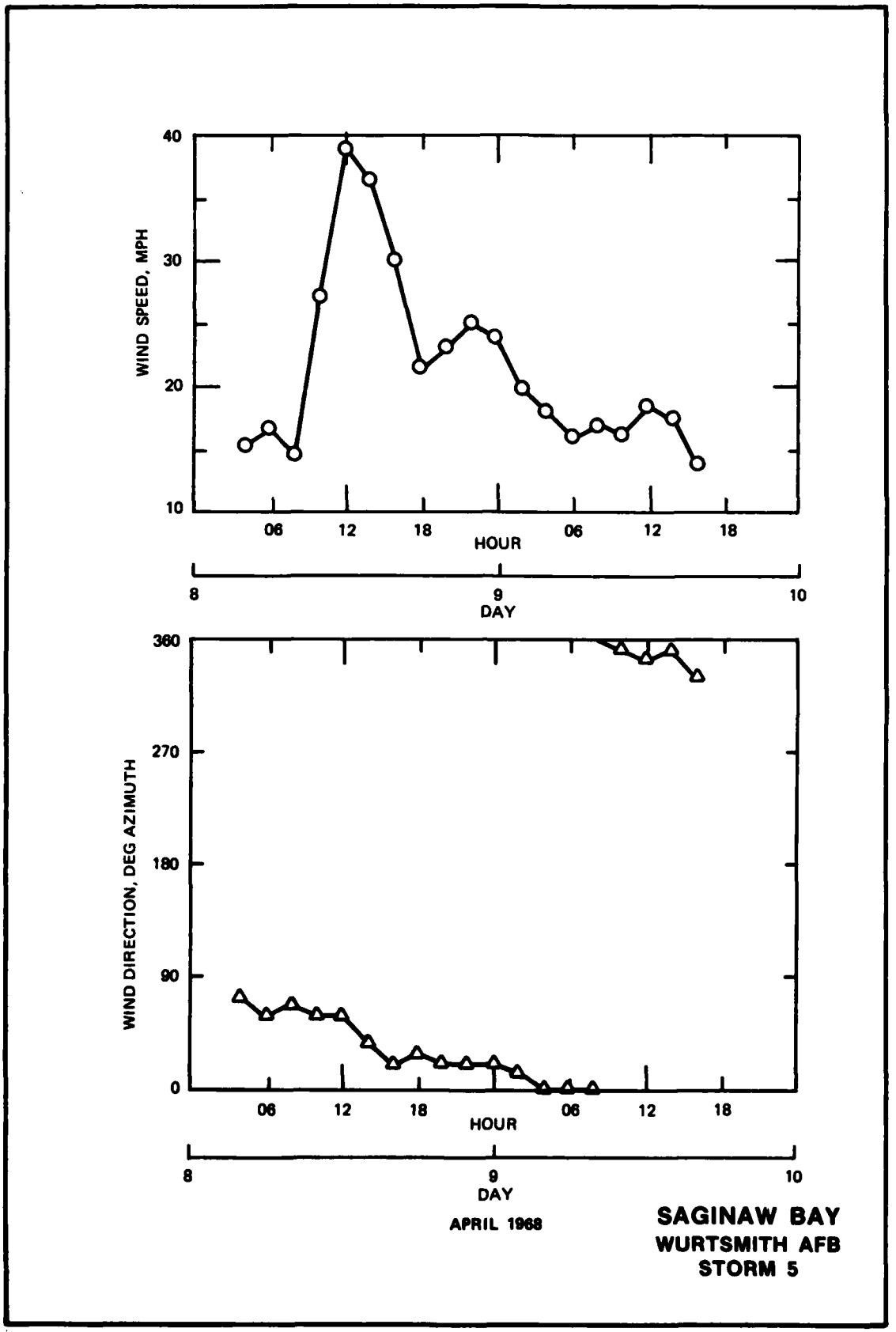


Figure A9. Wind data used for hindcast of 8-10 April 1968

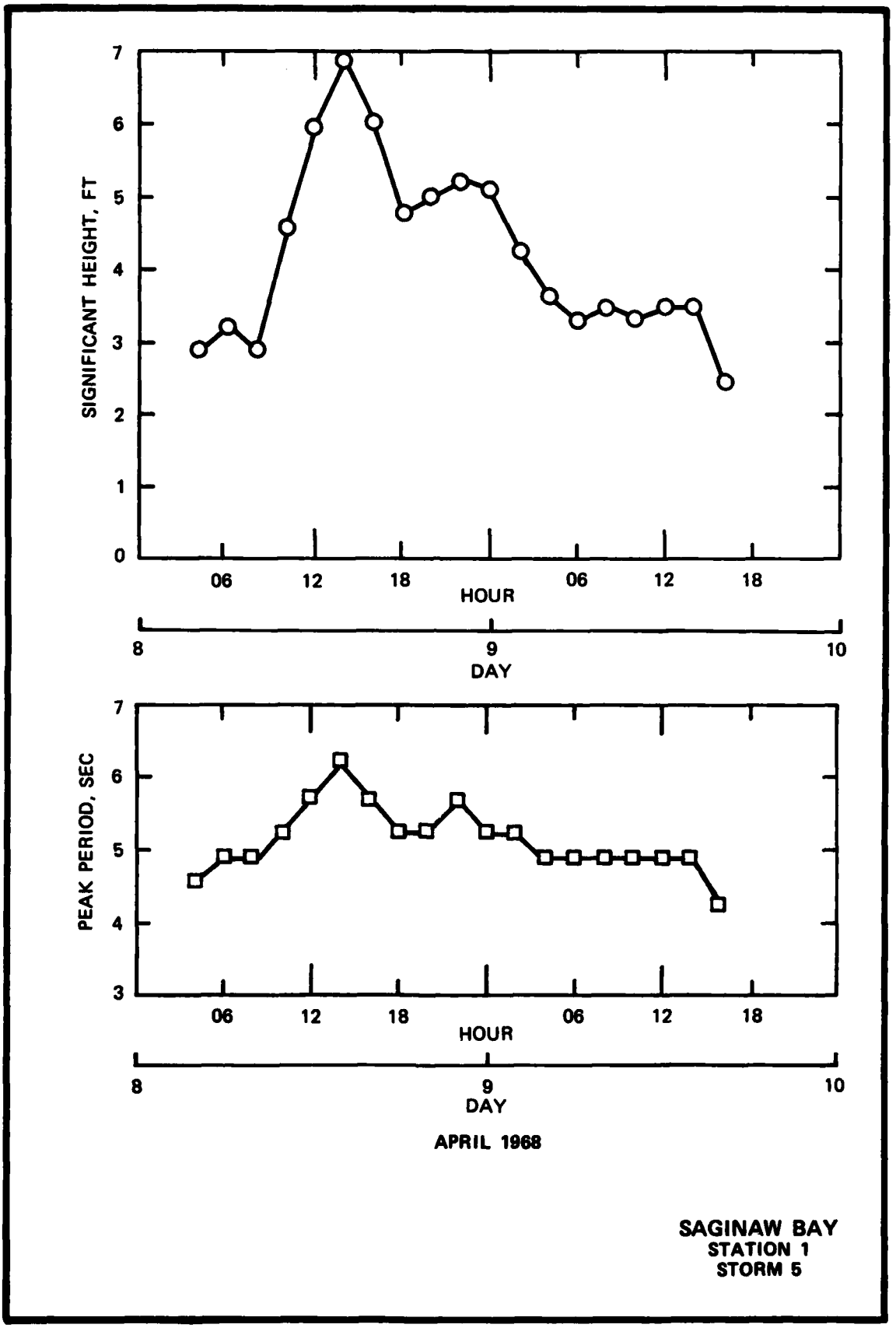


Figure A10. Hindcast significant wave height and peak wave period for storm of 8-10 April 1968

# APPENDIX B: NOTATION

| | |
|---|---|
| D | Height of wave sensor above the bottom |
| E | Final total energy at $F_i$ |
| $E_o$ | Total energy resulting from a wind speed |
| $E_s$ | Spectral energy density of the sea surface |
| $E(f_j)$ | Energy density at each discrete frequency band |
| E(f,h) THEORY | Saturated spectrum based on Equations 15 and 19 |
| E(f,h) WEIGHTED | Spectrum based on $E_o$ after wave growth |
| $E_1$ | Original total energy at $F_{i-1}$ |
| fc | Lower frequency bounding the total energy |
| $\tilde{f}_m$ | Nondimensional peak frequency |
| ff | Nondimensional friction factor |
| F | Fetch length |
| $F_i$ | Discrete fetch length |
| g | Acceleration due to gravity |
| h | Local water depth |
| $\bar{h}$ | Mean water depth along F |
| $h_i$ | Water depth at $F_i$ |
| $H_m$ | Maximum wave condition |
| $H_{m_0}$ | Significant wave height |
| $H'_{m_0}$ | Maximum significant height in a given storm |
| $H_{1/3}$ | Significant wave height |
| i | Increment counter |
| k | Local wave number |
| $k_i$ | Wave number $k_i = \frac{2\pi}{L_i}$ |
| K | Nonvarying parameters |
| $L_i$ | Wavelength evaluated for $f_m$ |
| NY | Duration if data base in years |
| P | Pressure response factor |
| Q | Dependent parameters |
| R | Storm rank |
| t | Time since wind began to blow |
| $t_{min}$ | Minimum duration condition |

| | |
|---|---|
| $T$ | Length of wave record |
| $T_p$ | Peak wave period |
| $T_R$ | Return period |
| $T_s$ | Significant wave period |
| $U$ | Wind speed |
| $\tilde{X}$ | Nondimensional fetch length |
| $\alpha$ | Phillips' equilibrium constant |
| $\Delta_t$ | Sampling interval |
| $\Delta F_i$ | Distance of wave travel within discrete fetch length |
| $\zeta_i$ | Independent parameters |
| $\sigma^2$ | Variance about the mean $H_{m_0}$ (or $\bar{H}_{m_0}$) |
| $\phi_f$ | Friction function, units of $T^4 - L^{-2}$ |
| $\phi(\omega_h)$ | Nondimensional function dependent on $\omega_h$ |

Subscripts

| | |
|---|---|
| s, p | Surface and pressure spectra, respectively |


FIL